

Article

Thermodynamic Analysis of Chemical Hydrogen Storage: Energetics of Liquid Organic Hydrogen Carrier Systems Based on Methyl-Substituted Indoles

Sergey V. Vostrikov ^{1,*}, Artemiy A. Samarov ², Vladimir V. Turovtsev ³, Peter Wasserscheid ^{4,5}, Karsten Müller ^{5,6} and Sergey P. Verevkin ^{7,8,*}

¹ Chemical-Technological Department, Samara State Technical University, 443100 Samara, Russia

² Department of Chemical Thermodynamics and Kinetics, Saint Petersburg State University, 198504 Saint Petersburg, Russia; samarov@yandex.ru

³ Department of Physics, Tver State Medical University, 170100 Tver, Russia; turtsma@mail.ru

⁴ Institute of Chemical Reaction Engineering, Friedrich-Alexander-Universität Erlangen-Nürnberg, Egerlandstr. 3, 91058 Erlangen, Germany; peter.wasserscheid@fau.de

⁵ Forschungszentrum Jülich GmbH, Helmholtz Institute Erlangen-Nürnberg for Renewable Energy (IEK-11), Egerlandstr. 3, 91058 Erlangen, Germany; karsten.mueller@uni-rostock.de

⁶ Institute of Technical Thermodynamics, University of Rostock, Albert-Einstein Str. 2, 18059 Rostock, Germany

⁷ Competence Centre CALOR of the Department Life, Light & Matter, Faculty of Interdisciplinary Research, University of Rostock, 18059 Rostock, Germany

⁸ Department of Physical Chemistry, Kazan Federal University, 420008 Kazan, Russia

* Correspondence: vosser@mail.ru (S.V.V.); sergey.verevkin@uni-rostock.de (S.P.V.)

Abstract: Liquid organic hydrogen carriers can store hydrogen in a safe and dense form through covalent bonds. Hydrogen uptake and release are realized by catalytic hydrogenation and dehydrogenation, respectively. Indoles have been demonstrated to be interesting candidates for this task. The enthalpy of reaction is a crucial parameter in this regard as it determines not only the heat demand for hydrogen release, but also the reaction equilibrium at given conditions. In this work, a combination of experimental measurements, quantum chemical methods and a group-additivity approach has been applied to obtain a consistent dataset on the enthalpies of formation of different methylated indole derivatives and their hydrogenated counterparts. The results show a namable influence of the number and position of methyl groups on the enthalpy of reaction. The enthalpy of reaction of the overall hydrogenation reaction varies in the range of up to 18.2 kJ·mol⁻¹ (corresponding to 4.6 kJ·mol(H₂)⁻¹). The widest range of enthalpy of reaction data for different methyl indoles has been observed for the last step (hydrogenation for the last double bond in the five-membered ring). Here a difference of up to 7.3 kJ·mol(H₂)⁻¹ between the highest and the lowest value was found.

Keywords: vapor pressure; enthalpy of vaporization; enthalpy of formation; structure–property relationships; quantum chemical calculations



Citation: Vostrikov, S.V.; Samarov, A.A.; Turovtsev, V.V.; Wasserscheid, P.; Müller, K.; Verevkin, S.P. Thermodynamic Analysis of Chemical Hydrogen Storage: Energetics of Liquid Organic Hydrogen Carrier Systems Based on Methyl-Substituted Indoles. *Materials* **2023**, *16*, 2924. <https://doi.org/10.3390/ma16072924>

Academic Editors: Alessandro Dell’Era and Erwin Ciro Zuleta

Received: 7 February 2023

Revised: 30 March 2023

Accepted: 31 March 2023

Published: 6 April 2023



Copyright: © 2023 by the authors. Licensee MDPI, Basel, Switzerland. This article is an open access article distributed under the terms and conditions of the Creative Commons Attribution (CC BY) license (<https://creativecommons.org/licenses/by/4.0/>).

1. Introduction

Chemical hydrogen storage and release processes are essential prerequisites for the implementation of a sustainable energy system [1]. The last decade has seen rapid growth in research activities on hydrogen storage materials. Reversible hydrogenation/dehydrogenation of aromatic compounds suitable as liquid organic hydrogen carriers (LOHCs) is considered a promising alternative to conventional hydrogen storage technologies. There are different types of hydrogen carriers that can be utilized as LOHCs. Sometimes substances that are irreversibly decomposed to hydrogen and carbon dioxide (such as formic acid or methanol) are included in the term [2]. However, the most promising materials are those that can be applied in multiple cycles. Chemical hydrogen storage with these LOHC systems is usually achieved by catalytic hydrogenation of a material containing unsaturated or

aromatic molecules (hydrogen uptake), which are then reversibly dehydrogenated on a catalyst, releasing the hydrogen that can be used subsequently [3,4]. The main advantage of LOHC-based hydrogen storage compared to, e.g., solid carrier materials is the fact that the hydrogen is stored in a liquid material whose physical properties are beneficial for handling in a fuel-like manner. For instance, the liquid nature of the material enables the pumping of the carrier and control of hydrogen release by removing the catalyst. Furthermore, the kinetics of hydrogen uptake and release are much better than those in metal hydrides. A slight disadvantage is the fact that hydrogen needs purification after release as small amounts of the carrier are evaporated.

Indole derivatives are considered as promising liquid organic hydrogen carriers for on-board hydrogen storage applications [5]. A property that makes indoles particularly attractive compared to other materials is the rather low enthalpy of reaction for hydrogen release. The indole derivatives are among the most common and important heterocycles in nature. The continuous development of routes to indoles has been a central theme in organic synthesis over the last century, which is commensurate with their importance [6]. Indole and its derivatives can be synthesized by a variety of conventional methods [7–9]. Moreover, the indole derivatives can also be biosynthesized [10].

The kinetics of hydrogenation/dehydrogenation reactions of methyl-indoles have been intensively studied in the recent past [11–13]. The kinetics of hydrogenation of 2-methyl-indole were studied over the Ru/Al₂O₃ (5 wt%) catalyst in the temperature range of 120–170 °C at a hydrogen pressure of 7 MPa. Reversible dehydrogenation was achieved with the same catalyst in 4 h at 190 °C [11].

The hydrogenation of 1-methylindole and the dehydrogenation of octahydro-1-methylindole were investigated over a 5 wt% Ru/Al₂O₃ catalyst. Hydrogenation with nearly 100% conversion and selectivity was easily achieved at 130 °C and 6.0 MPa. The successful dehydrogenation was performed in the temperature range of 160–190 °C [12].

Full hydrogenation of 1,2-dimethyl-indole can be realized at 140 °C and 7 MPa in 60 min over a 5 wt% Ru/Al₂O₃ catalyst. The stored hydrogen can be completely released via perhydro-1,2-dimethyl-indole dehydrogenation at 200 °C and 101 kPa within 60 min over the same catalyst [13].

For 2,3-dimethylindole, complete hydrogenation was achieved over 5 wt% Ru/Al₂O₃ at 190 °C and 7 MPa in 4 h. Dehydrogenation of perhydro-2,3-dimethylindole was successfully performed over 5 wt% Pd/Al₂O₃ at 180–210 °C and 101 kPa [14].

All these examples show the principle feasibility of hydrogenation/dehydrogenation cycles using methyl indole derivatives. However, the optimization of the technological processes requires extended thermodynamic data on LOHC systems consisting of both counterparts (hydrogen-lean material (indoles) and hydrogen-rich material (perhydrohydrogenated indoles)), which are the subject of the present work. The present work continues the series of our earlier thermodynamic work [3,15] on indole derivatives. In contrast to previous studies, which focused on intermediates and the general effects of substitution [4], this work focuses on the reversible hydrogenation/dehydrogenation reactions in the dimethylindole-based LOHC systems (see Figure 1).

The energetics of these reactions are essential for chemical engineering calculations and the optimization of the heat streams of technological processes. The standard molar enthalpies of chemical reactions, $\Delta_r H_m^0$, are calculated from the enthalpies of formation of reactants and products according to Hess's law, e.g., for the complete hydrogenation reaction of a methyl indole:

$$\Delta_r H_m^0 = \Delta_f H_m^0(\text{HR}) - \Delta_f H_m^0(\text{HL}) - \Delta_f H_m^0(\text{H}_2) = \Delta_f H_m^0(\text{HR}) - \Delta_f H_m^0(\text{HL}) \quad (1)$$

where $\Delta_f H_m^0(\text{HR})$ and $\Delta_f H_m^0(\text{HL})$ are the standard molar enthalpies of formation of the hydrogen-rich and hydrogen-lean counterparts of the LOHC system (for example 3-methyl-(H8)-indole as HR counterpart and 3-methyl-indole as HL counterpart).

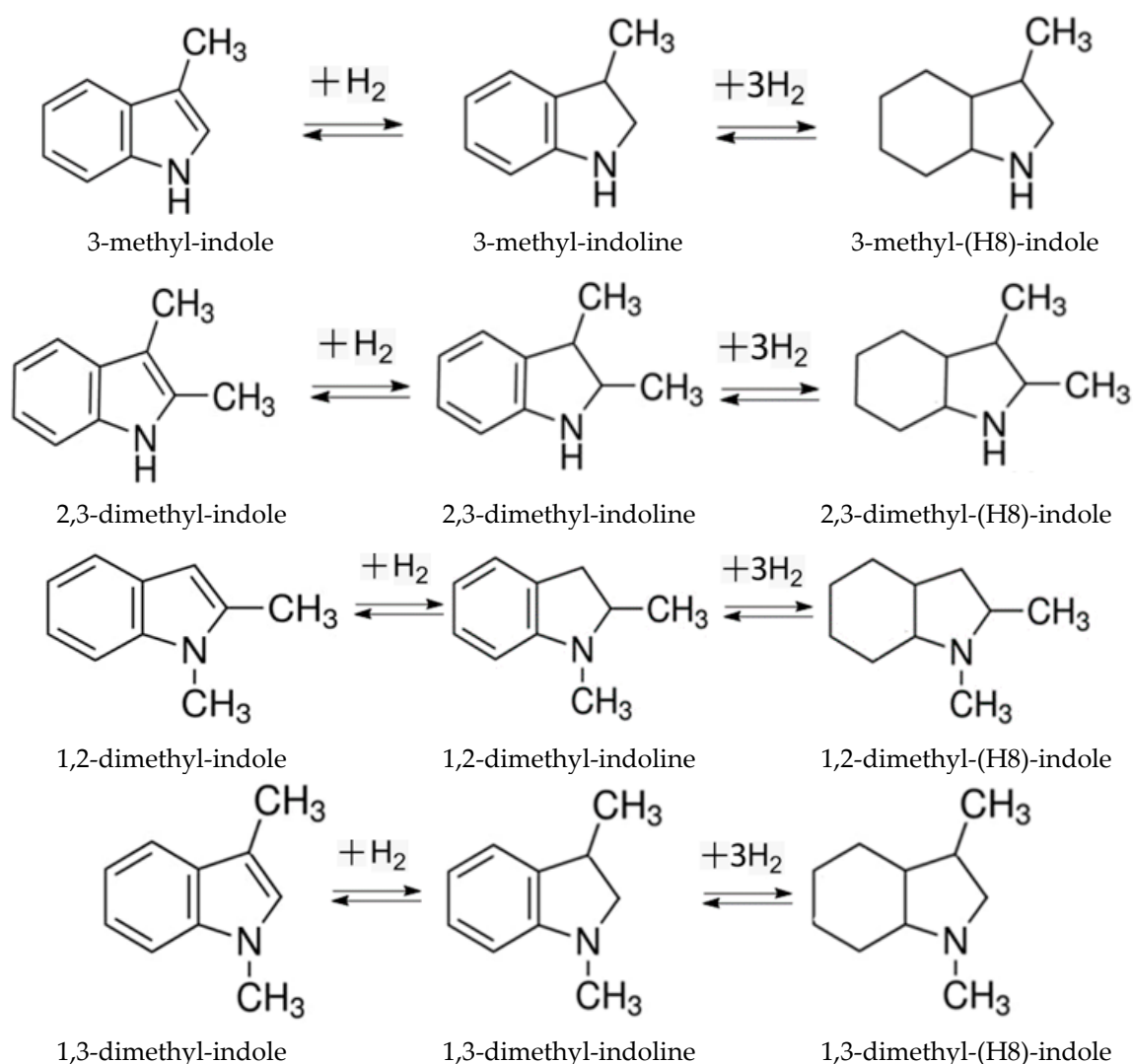


Figure 1. Reversible hydrogenation reactions in the methyl-indole-based LOHC systems studied in this work.

The catalytic process of reversible hydrogen storage and release is designed in the *liquid phase* at elevated temperatures and pressures; therefore, the standard molar enthalpies of formation, $\Delta_f H_m^\circ(\text{liq})$, of the LOHC counterparts in the *liquid phase* are needed. However, the purely experimental determination of all necessary thermodynamic data is thwarted by technical complications. In a number of our recent works [3,15], however, we have shown that a reasonable combination of experimental, empirical and quantum chemical calculations makes it possible to reduce the experimental effort without losing the reliability of the $\Delta_f H_m^\circ(\text{liq})$ -values.

The algorithm to derive the $\Delta_f H_m^\circ(\text{liq})$ -values consists of a few steps and is based on the general equations relating the thermochemical properties:

$$\Delta_f H_m^\circ(\text{liq}) = \Delta_f H_m^\circ(\text{g}) - \Delta_1^\circ H_m^\circ \quad (2)$$

$$\Delta_f H_m^\circ(\text{liq}) = \Delta_f H_m^\circ(\text{g}) - \left(\Delta_{\text{cr}}^\circ H_m^\circ - \Delta_{\text{cr}}^1 H_m^\circ \right) \quad (3)$$

where the standard molar vaporization enthalpies, $\Delta_1^\circ H_m^\circ$, the standard molar sublimation enthalpies, $\Delta_{\text{cr}}^\circ H_m^\circ$, and the standard molar fusion enthalpies, $\Delta_{\text{cr}}^1 H_m^\circ$, are usually measured by different experimental methods [16]. In thermochemistry, it is common to adjust all

enthalpies involved in Equations (1)–(3) to an arbitrary but common reference temperature. In this work, a reference temperature of $T = 298.15$ K was chosen.

Step I: In the first step, high-level quantum chemical (QC) methods of the G*-family (e.g., G3MP2 [17], G4 [18]) and the CBS-APNO [19] method are used to derive the gas-phase enthalpies of formation, $\Delta_f H_m^o(g, 298.15 \text{ K})$, for both HL and HR counterparts of the LOHC systems. In our experience [3,15], the results of these methods agree well with the available experimental gas-phase enthalpies of formations.

Step II: The vaporization enthalpies, $\Delta_1^g H_m^o(298.15 \text{ K})$ required for the calculations according to Equation (2), are collected from literature and validated with complementary measurements.

The sublimation enthalpies, $\Delta_{cr}^g H_m^o(298.15 \text{ K})$ required for the calculations according to Equation (3), are collected from literature and also validated with complementary measurements. The fusion enthalpies, $\Delta_{cr}^l H_m^o$, which are also needed for the calculation of the enthalpies of formation in the *liquid phase* according to Equation (3), can easily be measured by differential scanning calorimetry (DSC).

Step III: The vaporization enthalpies, $\Delta_1^g H_m^o(298.15 \text{ K})$ required for the calculations according to Equation (2), are often missing, especially for the alicyclic, hydrogen-rich materials. In such cases, $\Delta_1^g H_m^o(298.15 \text{ K})$ -values can be obtained from correlation with measurable physico-chemical properties (e.g., normal boiling temperatures or gas-chromatographic retention indices). These different types of correlations not only provide the missing values, but also cross-link the vaporization enthalpies of HL and HR materials to the network of reliable data and provide confidence in the evaluated numerical value. For such cases, we have also developed a “centerpiece” approach that is suitable for a reliable appraisal of the required thermodynamic data and is based on the principles of group additivity.

Step IV: The target enthalpies of formation of the HL and HR materials in *liquid phase* are derived according to Equations (2) and (3) and used in Equation (1) to estimate the hydrogenation/dehydrogenation enthalpies of the LOHC systems and to analyze how the structural features affect the energetics of this process.

The “step-by-step” evaluation of the thermodynamic properties of the HR and HL materials leading to the energetics of hydrogenation/dehydrogenation reactions with methyl-indole derivatives and the analysis of these results are the focus of this work.

2. Methods

2.1. Materials

Samples of 3-methyl-indole and 1,2-dimethyl-indole were of commercial origin (see Table S1) with purities of 0.99 mass fraction as given in the specification. Prior to the experiment, the samples were purified using fractional vacuum sublimation. Purities were determined using a gas chromatograph equipped with a flame ionization detector and a capillary column HP-5 (stationary phase crosslinked 5% PH ME silicone, column length of 30 m, inside diameter of 0.32 mm, film thickness of 0.25 μm). The analysis was performed with the temperature program $T = 353 \text{ K}$ for 30 s followed by a heating rate of 10 $\text{K}\cdot\text{min}^{-1}$ to $T = 523 \text{ K}$. No contamination (greater than the mass fraction 0.0009) could be detected in the samples used for the thermochemical measurements.

2.2. Theoretical and Experimental Thermochemical Methods

The theoretical gas-phase enthalpies of methyl-indoles were calculated using the composite QC methods [16–19] from the Gaussian 16 suitcase software [20]. The H_{298} -values were finally converted to the $\Delta_f H_m^o(g, 298.15 \text{ K})_{\text{theor}}$ values and discussed. For quantum chemical calculations, the most stable conformer of each compound was selected. The well-established assumption “rigid rotator–harmonic oscillator” was used for the quantum chemical calculations. Details on the calculation methods have been reported elsewhere [21].

The transpiration method [22] was applied to measure the vapor pressures of 3-methyl-indole and 1,2-dimethyl-indole at different temperatures. The standard molar

enthalpies of sublimation, $\Delta_{\text{cr}}^{\text{g}}H_{\text{m}}^{\circ}$, for 3-methyl-indole and 1,2-dimethyl-indole, as well as the standard molar enthalpy of vaporization, $\Delta_{\text{l}}^{\text{g}}H_{\text{m}}^{\circ}$, of 1,2-dimethyl-indole were derived from the temperature dependencies of the vapor pressures. The details of the experimental technique are given in the Electronic Support Information (ESI).

3. Results

3.1. Step I: Gas-Phase Standard Molar Enthalpies of Formation: Theory and Experiment

Quantum chemical methods have become a valuable tool to obtain the *theoretical* $\Delta_{\text{f}}H_{\text{m}}^{\circ}(\text{g}, 298.15 \text{ K})$ -values with “chemical accuracy” (conventionally at the level of 4–5 $\text{kJ}\cdot\text{mol}^{-1}$) [23]. In our recent work [3], we tested the G4 composite method by comparing the results with experimental data obtained by high-precision combustion calorimetry and vapor pressure measurements (see Table 1).

Table 1. Compilation of thermochemical data for indole derivatives at $T = 298.15 \text{ K}$ ($p = 0.1 \text{ MPa}$, in $\text{kJ}\cdot\text{mol}^{-1}$)^a.

Compound	$\Delta_{\text{f}}H_{\text{m}}^{\circ}(\text{cr,l})$	$\Delta_{\text{cr,l}}^{\text{g}}H_{\text{m}}^{\circ}$	$\Delta_{\text{f}}H_{\text{m}}^{\circ}(\text{g})_{\text{exp}}$	$\Delta_{\text{f}}H_{\text{m}}^{\circ}(\text{g})_{\text{G4}}$ ^b
1	2	3	4	5
indole (cr) [3]	87.2 ± 0.9	75.3 ± 0.4	162.5 ± 1.0	160.4
indoline (liq) [3]	60.0 ± 0.9	60.8 ± 0.9	120.8 ± 1.3	117.6
H8-indole (liq) [3]	-117.5 ± 1.8	53.5 ± 0.7	-64.0 ± 1.9	-63.5
2-methyl-indole (cr) [3]	36.1 ± 1.3	85.3 ± 0.4	121.4 ± 1.4	120.2
2-methyl-indoline [3]	17.2 ± 1.9	63.0 ± 0.4	80.2 ± 1.9	79.4
2-methyl-H8-indole [3]	-157.1 ± 2.1	57.8 ± 0.8	-99.3 ± 2.2	-100.4
3-methyl-indole (cr)	47.4 ± 2.3 [24]	81.3 ± 0.5 ^c	128.7 ± 2.4	126.0 ^d
2,3-dimethyl-indole (cr)	4.2 ± 1.0 [25]	86.0 ± 0.6 ^c	90.2 ± 1.2	86.6 ^d

^a The uncertainties in this table are given as 2 times the standard deviation. ^b Calculated in [3] with the G4 method using the atomization procedure. ^c Evaluated in this work. ^d Calculated in this work with the G4 method using the atomization procedure.

As can be seen from this table, the deviation between the G4 method and experimental results is no more than 2–3 $\text{kJ}\cdot\text{mol}^{-1}$, which is even better than the claimed “chemical accuracy”. However, in this work, the G3MP2 and CBS-APNO methods were tested additionally to estimate the *theoretical* $\Delta_{\text{f}}H_{\text{m}}^{\circ}(\text{g}, 298.15 \text{ K})$ -value of 3-methyl-indole as an example. The simultaneous use of several methods helps to avoid possible systematic errors in the calculations. Stable conformers of 3-methyl-indole were found using a CREST (Conformer-Rotamer Ensemble Sampling Tool) computer code [26] and optimized using the B3LYP/6-31g(d,p) method [27]. Since the structures of the 3-methyl indole conformers are flat, the energetic differences do not exceed 1 $\text{kJ}\cdot\text{mol}^{-1}$. Therefore, the high-level calculations were performed only for the most stable conformer. The energy E_0 and the enthalpy H_{298} of the most stable conformer were finally calculated by using the high-level quantum chemical methods. The H_{298} -values were converted to the standard molar enthalpies of formation $\Delta_{\text{f}}H_{\text{m}}^{\circ}(\text{g}, 298.15 \text{ K})_{\text{AT}}$ by using the atomization (AT) reaction:



In addition, the H_{298} enthalpies of 3-methyl-indole were converted to the enthalpies of formation using the enthalpies of the homodesmotic reactions shown in Figure 2.

To derive the *theoretical* $\Delta_{\text{f}}H_{\text{m}}^{\circ}(\text{g}, 298.15 \text{ K})$, the experimental enthalpies of formation of the homodesmotic reaction participants were used. They are compiled in Table S2. The quantum chemical reaction enthalpies are given in Table S3. The resulting $\Delta_{\text{f}}H_{\text{m}}^{\circ}(\text{g}, 298.15 \text{ K})$ -values for each reaction are given in Table 2, as calculated by the methods G4, G3MP2 and CBS-APNO.

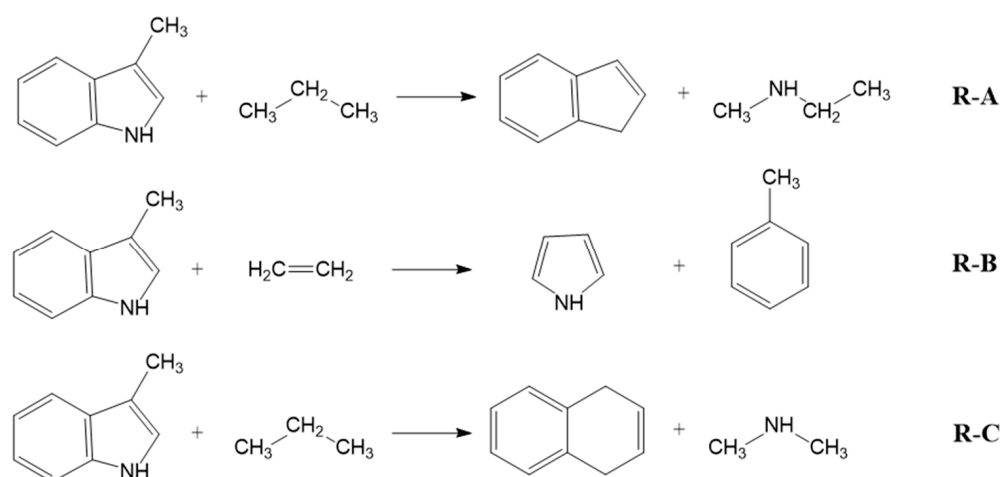


Figure 2. The homodesmotic reactions used to convert the H_{298} -values to the *theoretical* standard molar enthalpies of formation $\Delta_f H_m^0(\text{g}, 298.15 \text{ K})$.

Table 2. Results of the quantum chemical calculations of $\Delta_f H_m^0(\text{g}, 298.15 \text{ K})$ for 3-methyl-indole with different methods at $T = 298.15 \text{ K}$ ($p^\circ = 0.1 \text{ MPa}$, in $\text{kJ}\cdot\text{mol}^{-1}$).

Method	(AT)	R-A	R-B	R-C	Exp. [Table 1]
G4 ^a	126.0	126.6	125.6	126.6	128.7 ± 2.4
G3MP2 ^b	122.9	129.1	127.2	129.3	
CBS-APNO ^c	125.1	127.8	125.4	127.5	

^a Calculated according to the G4 method using atomization reaction Equation (4) and the homodesmotic reactions shown in Figure 2. The expanded uncertainties are assessed to be $\pm 3.5 \text{ kJ}\cdot\text{mol}^{-1}$ [18]. ^b Calculated according to the G3MP2 method using atomization reaction Equation (4) and the homodesmotic reactions shown in Figure 2. The expanded uncertainties are assessed to be $\pm 4.1 \text{ kJ}\cdot\text{mol}^{-1}$ [17]. ^c Calculated according to the CBS-APNO method using atomization reaction Equation (4) and the homodesmotic reactions shown in Figure 2. The expanded uncertainties are assessed to be $\pm 4.1 \text{ kJ}\cdot\text{mol}^{-1}$ [19].

As shown in Table 2, the theoretical enthalpies of formation of 3-methyl-indole calculated by G4, G3MP2 and CBS-APNO using atomization and homodesmotic reactions are quite close to the experimental value $\Delta_f H_m^0(\text{g}, 298.15 \text{ K})_{\text{exp}} = 128.7 \pm 2.4 \text{ kJ}\cdot\text{mol}^{-1}$ (see Table 1). In particular, the results of the G4 method are remarkably consistent, regardless of the type of reaction used to derive the gas-phase enthalpy of formation. Furthermore, the results of the G4 calculations for the series of indole derivatives compiled in Table 1 show very good agreement with the experimental data, even when the simplest atomization procedure, according to Equation (4), was used. In order to reduce the computational effort for the indole derivatives of interest in this study (see Figure 1), the calculations of the theoretical gas-phase enthalpies of formation were therefore only carried out using the G4 method and the atomization procedure. The structures of the most stable conformers and the resulting $\Delta_f H_m^0(\text{g}, 298.15 \text{ K})_{\text{G4}}$ -values for methyl- and dimethyl-indole derivatives are listed in Table 3.

The gas-phase enthalpies of formation of methylindoles calculated in Table 3 can now be substituted into Equations (2) and (3) to derive the hydrogenation reaction enthalpies for the LOHC systems based on methylindole derivatives.

Table 3. Structures of the most stable conformers and the G4 calculated gas-phase enthalpies of formation $\Delta_f H_m^0(g)_{G4}$ at $T = 298.15$ K ($p^\circ = 0.1$ MPa) for indole derivatives (in $\text{kJ}\cdot\text{mol}^{-1}$).

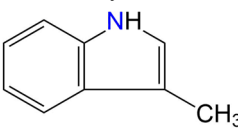
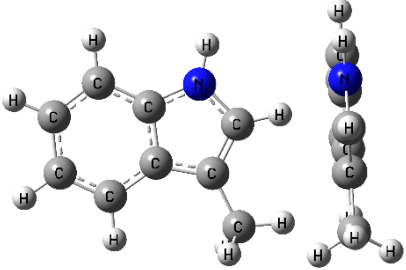
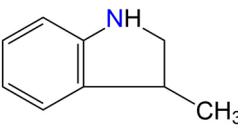
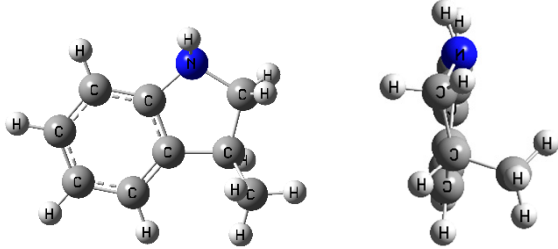
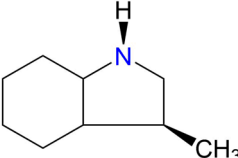
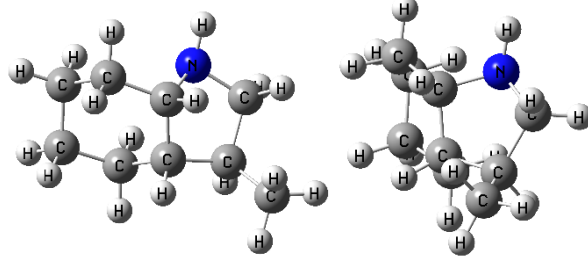
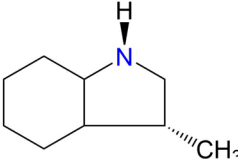
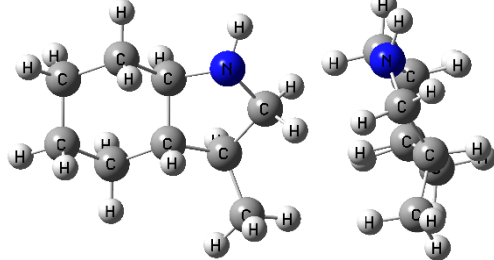
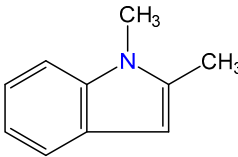
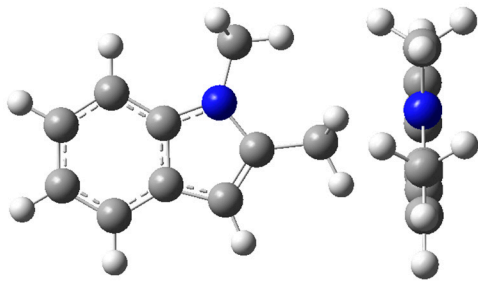
Indole	Structures	$\Delta_f H_m^0(g)_{G4}^a$
<p>3-methyl-indole</p> 		126.0
<p>3-methyl-indoline</p> 		85.8
<p>cis-3-methyl-(H8)-indole</p> 		−93.7
<p>trans-3-methyl-(H8)-indole</p> 		−93.8
<p>1,2-dimethylindole</p> 		111.4

Table 3. Cont.

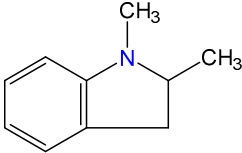
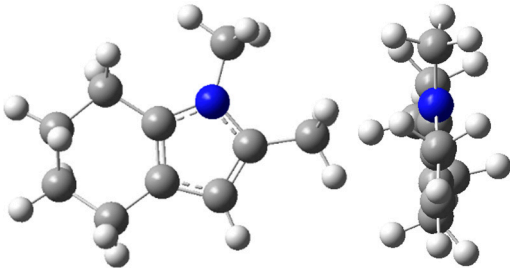
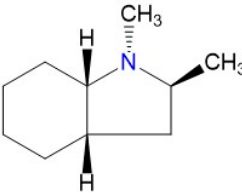
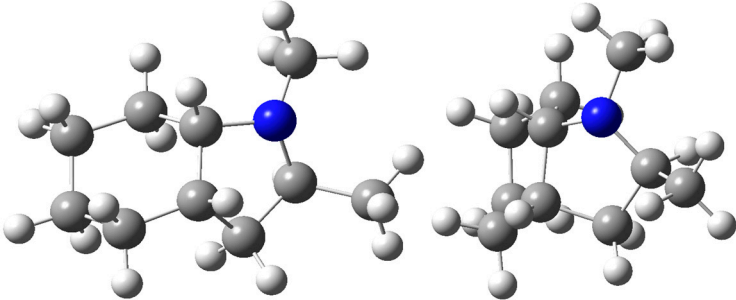
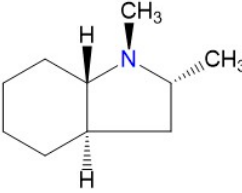
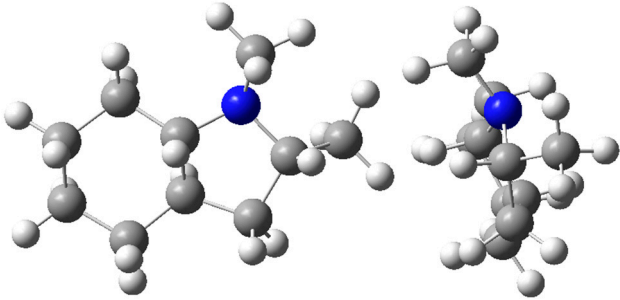
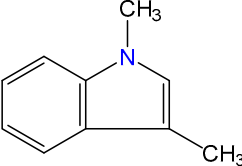
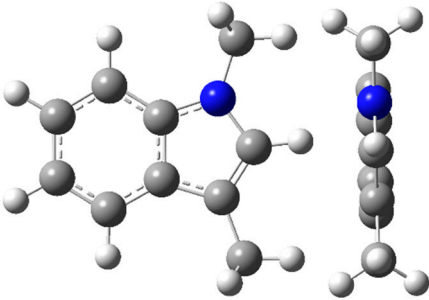
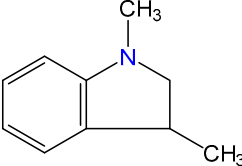
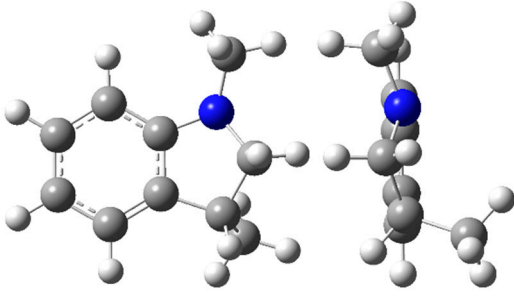
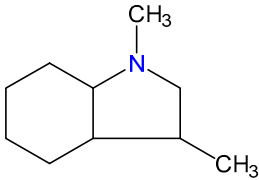
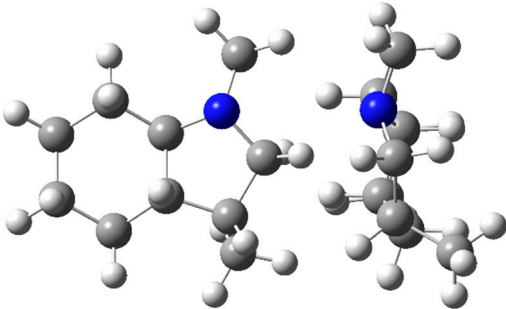
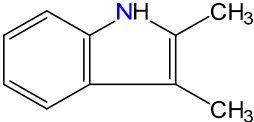
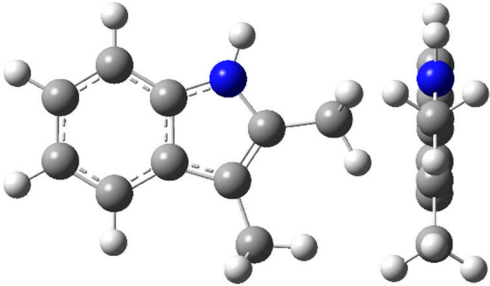
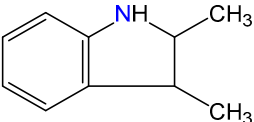
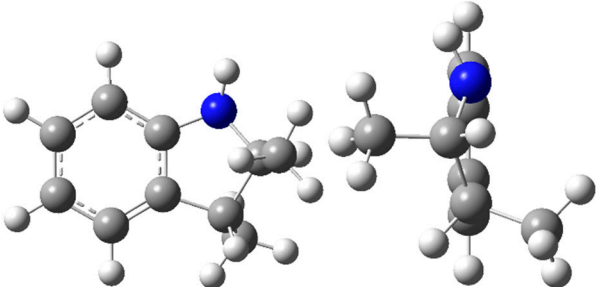
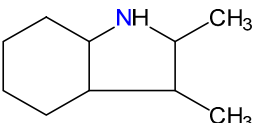
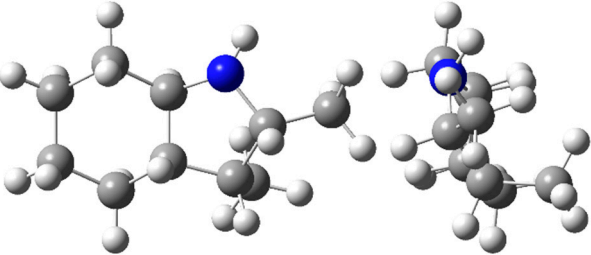
Indole	Structures	$\Delta_f H_m^0(\text{g})_{\text{G4}}^a$
1,2-dimethyl-indoline 		72.8
cis-1,2-dimethyl-(H8)-indole 		-105.5
trans-1,2-dimethyl-(H8)-indole 		-113.0
1,3-dimethylindole 		116.3
1,3-dimethyl-indoline 		74.6

Table 3. Cont.

Indole	Structures	$\Delta_f H_m^0(\text{g})_{\text{G4}}^a$
1,3-dimethyl-(H8)-indole 		−102.4
2,3-dimethylindole 		86.6
2,3-dimethyl-indoline 		47.0
2,3-dimethyl-(H8)-indole 		−120.9

^a Calculated according to the G4 method using the atomization procedure.

3.2. Step II: Vaporization Enthalpies of Indole Derivatives

3.2.1. Experimental Vapor Pressures

3-Methyl-indole and 1,2-dimethyl-indole are solids at room temperature with respective melting points of 368.0 K and 330.7 K, as given in Table S4. Moreover, for 3-methyl-indole, a solid–solid phase transition was observed at 316.8 K [4]. Therefore, for the correct interpretation of the phase transition data at the reference temperature $T = 298.15$ K (see Table S4), the sublimation enthalpy of 3-methylindole was measured below the phase transition temperature 316.8 K (see Table S4). The experimental dependences of the vapor

pressures, p_i , on temperature measured in this work for 3-methyl-indole and 1,2-dimethyl-indole (see Table 4) were correlated by the following equation [22]:

$$R \times \ln(p_i/p_{ref}) = a + \frac{b}{T} + \Delta_{cr,l}^g C_{p,m}^o \times \ln\left(\frac{T}{T_0}\right), \quad (5)$$

where $\Delta_{cr,l}^g C_{p,m}^o$ is the difference between the molar heat capacities of the gas and the crystal (or liquid) phases (see Table S5), a and b are adjustable parameters, $R = 8.31446 \text{ J}\cdot\text{K}^{-1}\cdot\text{mol}^{-1}$ is the molar gas constant, and the reference pressure $p_{ref} = 1 \text{ Pa}$. The arbitrary temperature T_0 given in Equation (5) was chosen to be $T_0 = 298.15 \text{ K}$. The results of the vapor pressure measurements using the transpiration method are shown in Table 4.

Experimental vapor pressures have been used to obtain the enthalpies of sublimation/vaporization using the following equation:

$$\Delta_{cr,l}^g H_m^o(T) = -b + \Delta_{cr,l}^g C_{p,m}^o \times T \quad (6)$$

Table 4. Results of transpiration method for methyl-indole derivatives: absolute vapor pressures p , standard molar sublimation/vaporization enthalpies and standard molar sublimation/vaporization entropies.

$T/$ K^a	$m/$ mg^b	$V(\text{N}_2)^c/$ dm^3	$T_a/$ K^d	Flow/ $\text{dm}^3\cdot\text{h}^{-1}$	$p/$ Pa^e	$u(p)/$ Pa^f	$\Delta_{cr,l}^g H_m^o(T)/$ $\text{kJ}\cdot\text{mol}^{-1}$	$\Delta_{l,cr}^g S_m^o(T)/$ $\text{J}\cdot\text{K}^{-1}\cdot\text{mol}^{-1}$
3-methyl-indole: $\Delta_{cr}^g H_m^o(298.15 \text{ K}) = (81.4 \pm 0.6) \text{ kJ}\cdot\text{mol}^{-1}$								
$\ln(p/p_{ref}) = \frac{296.4}{R} - \frac{89468.6}{RT} - \frac{27.1}{R} \ln \frac{T}{298.15}; p_{ref} = 1 \text{ Pa}$								
285.2	1.08	143.6	296.2	4.03	0.14	0.01	81.7	174.7
288.2	1.13	104.3	296.2	4.03	0.20	0.01	81.7	174.4
290.2	1.31	93.58	296.2	4.03	0.26	0.01	81.6	174.4
293.2	1.26	64.12	298.2	4.05	0.37	0.01	81.5	174.2
298.2	1.53	44.26	298.2	2.95	0.65	0.02	81.4	173.7
308.2	1.60	16.20	296.2	4.05	1.85	0.05	81.1	172.6
315.8	1.29	6.038	296.2	4.03	4.01	0.11	80.9	172.0
1,2-dimethyl-indole: $\Delta_{cr}^g H_m^o(298.15 \text{ K}) = (83.2 \pm 0.7) \text{ kJ}\cdot\text{mol}^{-1}$								
$\ln(p/p_{ref}) = \frac{307.8}{R} - \frac{92463.2}{RT} - \frac{31.1}{R} \ln \frac{T}{298.15}; p_{ref} = 1 \text{ Pa}$								
298.2	2.12	47.790	293.2	3.19	0.75	0.02	83.2	180.9
302.2	0.84	11.90	293.2	5.10	1.19	0.03	83.1	180.6
306.2	0.83	7.653	293.2	5.10	1.81	0.05	82.9	180.1
310.2	0.85	5.102	293.2	5.10	2.81	0.08	82.8	179.9
312.2	0.76	3.797	293.2	5.06	3.36	0.09	82.8	179.5
314.2	0.34	1.367	293.2	4.10	4.13	0.11	82.7	179.3
314.2	0.72	2.953	293.2	5.06	4.09	0.11	82.7	179.2
316.2	0.81	2.700	293.2	5.06	5.06	0.15	82.6	179.1
318.2	0.62	1.709	293.2	4.10	6.13	0.18	82.6	178.9
320.2	0.73	1.645	293.2	5.06	7.48	0.21	82.5	178.7
322.2	0.75	1.367	293.2	4.10	9.18	0.25	82.4	178.6
324.2	0.94	1.435	293.2	5.06	10.94	0.30	82.4	178.3
326.2	1.08	1.367	293.2	4.10	13.25	0.36	82.3	178.2

Table 4. Cont.

$T/$ K ^a	$m/$ mg ^b	$V(N_2)$ ^c / dm ³	$T_a/$ K ^d	Flow/ dm ³ ·h ⁻¹	$p/$ Pa ^e	$u(p)/$ Pa ^f	$\Delta_{cr,l}^g H_m^o(T)/$ kJ·mol ⁻¹	$\Delta_{l,cr}^g S_m^o(T)/$ J·K ⁻¹ ·mol ⁻¹
1,2-dimethyl-indole: $\Delta_{cr,l}^g H_m^o(298.15\text{ K}) = (67.6 \pm 0.7)\text{ kJ}\cdot\text{mol}^{-1}$								
$\ln(p/p_{ref}) = \frac{300.8}{R} - \frac{88718.3}{RT} - \frac{70.8}{R} \ln \frac{T}{298.15}; p_{ref} = 1\text{ Pa}$								
331.2	1.98	1.543	293.2	2.06	21.59	0.56	65.3	126.9
334.2	1.91	1.200	293.2	2.06	26.66	0.69	65.1	126.3
338.2	1.76	0.857	293.2	2.06	34.43	0.89	64.8	125.3
342.2	1.85	0.686	293.2	2.06	45.34	1.16	64.5	124.5
346.2	2.45	0.698	293.2	2.09	59.00	1.50	64.2	123.7
350.2	2.02	0.441	293.2	1.06	76.91	1.95	63.9	123.0
354.2	2.07	0.353	293.2	1.06	98.12	2.48	63.6	122.1
358.2	2.51	0.344	293.2	1.06	122.29	3.08	63.4	121.2
362.2	2.63	0.282	293.2	1.06	155.94	3.92	63.1	120.4
366.2	5.08	0.423	293.2	1.01	201.38	5.06	62.8	119.9
370.2	3.75	0.254	293.2	1.01	247.93	6.22	62.5	119.0

^a Saturation temperature measured with the standard uncertainty ($u(T) = 0.1\text{ K}$). ^b Mass of transferred sample condensed at $T = 243\text{ K}$. ^c Volume of nitrogen ($u(V) = 0.005\text{ dm}^3$) used to transfer m ($u(m) = 0.0001\text{ g}$) of the sample. Uncertainties are given as standard uncertainties. ^d T_a is the temperature of the soap bubble meter used for measurement of the gas flow. ^e Vapor pressure at temperature T , calculated from the m and the residual vapor pressure at the condensation temperature calculated by an iteration procedure. ^f Standard uncertainties were calculated with $u(p_i/\text{Pa}) = 0.005 + 0.025(p_i/\text{Pa})$ for pressures below 5 Pa and with $u(p_i/\text{Pa}) = 0.025 + 0.025(p_i/\text{Pa})$ for pressures from 5 to 3000 Pa. The standard uncertainties for T , V , p and m correspond to a confidence level of 68.3%. Uncertainties of the sublimation/vaporization enthalpies $U(\Delta_{cr,l}^g H_m^o)$ are the expanded uncertainty (level of confidence: 95%, corresponding to 2 times the standard deviation) calculated according to procedures described elsewhere [28]. Uncertainties include uncertainties from the experimental conditions and the fitting equation, vapor pressures and uncertainties from adjustment of vaporization enthalpies to the reference temperature $T = 298.15\text{ K}$.

Experimental vapor pressures temperature dependences were also used to derive the sublimation/vaporization entropies at temperatures T by using the following equation:

$$\Delta_{cr,l}^g S_m^o(T) = \Delta_{cr,l}^g H_m^o/T + R \times \ln(p_i/p^o) \quad (7)$$

with $p^o = 0.1\text{ MPa}$. Coefficients a and b of Equation (5), $\Delta_{cr,l}^g H_m^o(T)$ and $\Delta_{cr,l}^g S_m^o(T)$ values are collected in Table 4. According to general practice, all thermochemical quantities must be presented at the reference temperature $T = 298.15\text{ K}$. Details of the temperature adjustment are given in Table S5. The resulting sublimation/vaporization enthalpies at the reference temperature $T = 298.15\text{ K}$ are given in Table 5, column 5.

Table 5. Compilation of available enthalpies of sublimation/vaporization $\Delta_{cr,l}^g H_m^o$ of methyl-substituted indole derivatives.

Compound/CAS	Method ^a	T-Range	$\Delta_{cr,l}^g H_m^o(T_{av})$	$\Delta_{cr,l}^g H_m^o(298.15\text{ K})$ ^b	Ref.
		K	kJ·mol ⁻¹	kJ·mol ⁻¹	
3-methyl-indole (cr II) 83-34-1	n/a	288–333	83.3 ± 2.0	(83.6 ± 2.1) ^c	[29]
	DC	349.9	83.0 ± 1.9	(90.4 ± 2.4)	[24]
	T	285.2–315.8	81.4 ± 0.6	81.4 ± 0.6	Table 4
	FT			81.2 ± 0.7	Table S4
				81.3 ± 0.5^d	average
3-methyl-indole (cr I)	T	317.2–364.2	78.0 ± 0.4	79.3 ± 0.5	[3]
3-methyl-indole (liq)	n/a	368.2–539.4	63.7 ± 1.0	73.8 ± 2.2	[30]
	FT			69.8 ± 0.6	Table S4
	FT			70.0 ± 1.3	Table S4
	J_x			70.2 ± 1.5	[3]
	J_{Lee}			70.2 ± 1.5	[3]
				70.1 ± 0.5^d	average

Table 5. Cont.

Compound/CAS	Method ^a	T-Range	$\Delta_{\text{cr,l}}^{\text{g}} H_{\text{m}}^{\circ}(T_{\text{av}})$	$\Delta_{\text{cr,l}}^{\text{g}} H_{\text{m}}^{\circ}(298.15 \text{ K})$ ^b	Ref.
		K	$\text{kJ}\cdot\text{mol}^{-1}$	$\text{kJ}\cdot\text{mol}^{-1}$	
2,3-dimethyl-indole (cr) 91-55-4				86.0 ± 0.6	[3]
2,3-dimethyl-indole (liq)				75.2 ± 1.0	[3]
1,2-dimethyl-indole (cr)	T	298.2–326.2	82.8 ± 0.6	83.2 ± 0.7	Table 4
1,2-dimethyl-indole (liq) 875-79-6	T	331.2–370.2	64.0 ± 0.6	67.6 ± 0.7	Table 4
	FT			69.9 ± 1.3	Table S4
	J_{Lee}			67.6 ± 1.0	Table S7
				67.6 ± 0.6 ^d	average
1,3-dimethyl-indole (liq) 875-30-9	BP	335–533	58.7 ± 1.2	67.9 ± 1.2	Table S6
				T_{b}	67.3 ± 1.0
				67.5 ± 0.8 ^d	average
3-methyl-indoline (liq) 4375-15-9	BP	329–525	56.6 ± 0.9	65.1 ± 1.9	Table S6
	J_{x}			63.2 ± 1.0	Table 6
	J_{x}			64.1 ± 1.5	[3]
	CP			63.9 ± 1.0	this work
				63.8 ± 0.6 ^d	average
2,3-dimethyl-indoline (liq) 22120-50-9	BP	398–523	54.9 ± 3.0	67.1 ± 3.9	Table S6
	CP			66.1 ± 1.0	this work
				66.2 ± 1.0 ^d	average
1,2-dimethyl-indoline (liq) 26216-93-3	BP	314–501	53.1 ± 1.8	60.8 ± 2.3	Table S6
	CP			60.5 ± 1.0	this work
				60.5 ± 0.9 ^d	average
1,3-dimethyl-indoline (liq) 39891-78-6	BP	322–523	51.5 ± 1.6	60.0 ± 2.3	Table S6
	CP			60.5 ± 1.0	this work
				60.4 ± 0.9 ^d	average
3-methyl-(H8)-indole (liq) 85158-21-0	J_{x}			58.0 ± 1.0	Table 6
				58.1 ± 1.0	[3]
				58.0 ± 0.7 ^d	average
2,3-dimethyl-(H8)-indole (liq) 1394248-06-6	J_{x}			61.2 ± 1.0	[3]
1,2-dimethyl-(H8)-indole (liq) 87401-40-9	CP			52.3 ± 1.0	this work
1,3-dimethyl-(H8)-indole (liq) 87401-41-0	CP			52.3 ± 1.0	this work

^a Techniques: DC = drop calorimetry; T = transpiration method; FT = derived as the difference of sublimation and fusion enthalpies (see Table S4); J_{x} —derived from correlation with Kovats indices BP = derived from boiling points at different temperatures available in the literature (see Table S6); J_{Lee} —derived from correlation with Lee indices (see Table S7); n/a—method is not available; CP = derived using the “centerpiece” approach (see text); T_{b} = derived from correlation of vaporization enthalpies with the normal boiling points (see text). ^b Uncertainty of the sublimation/vaporization enthalpy $U(\Delta_{\text{cr,l}}^{\text{g}} H_{\text{m}}^{\circ})$ is the expanded uncertainty (0.95 level of confidence, $k = 2$) calculated according to a procedure described elsewhere [28]. It includes uncertainties from the experimental conditions, uncertainties of vapor pressure, uncertainties from the fitting equation and uncertainties from temperature adjustment to $T = 298.15 \text{ K}$. ^c The phase transition at $T_{\text{tr}} = 316.8 \text{ K}$ and enthalpy $\Delta_{\text{cr,l}}^{\text{cr,l}} H_{\text{m}}^{\circ} = 2.7 \pm 0.6 \text{ kJ}\cdot\text{mol}^{-1}$ was reported in our previous work [3]. ^d Weighted mean value. Values in parenthesis were excluded from the calculation of the mean. Values in bold are recommended for further thermochemical calculations.

The literature on vapor pressures of methyl indoles is sparse. The two sets found in the compilations [29,30] were approximated according to Equation (5), and the vaporization enthalpies are given in Table 5 for comparison. The uncertainties in the temperature adjustment of these enthalpies to the reference temperature $T = 298.15 \text{ K}$ were estimated to account for 20% of the total adjustment.

3.2.2. Evaluation of the Vaporization Enthalpies by Consistency of Phase Transitions Solid–Gas, Liquid–Gas and Solid–Liquid

For 3-methylindole, a solid–solid phase transition from phase II to phase I was observed at $\Delta T_{\text{trs}} = 316.8$ K [3]. The energetics of phase transition $\Delta_{\text{phase II}}^{\text{phase I}} H_{\text{m}}^{\circ} = 2.7 \pm 0.6$ kJ·mol^{−1} was measured at ΔT_{trs} [3]. The enthalpy of fusion of the phase I of 3-methyl-indole $\Delta_{\text{cr}}^{\text{I}} H_{\text{m}}^{\circ}(T_{\text{fus}}) = 11.6 \pm 0.5$ kJ·mol^{−1} (see Table S4) was measured in our previous work [3]. The total energetics of phase transitions below melting point for this compound was calculated as the sum of $\Delta_{\text{phase II}}^{\text{phase I}} H_{\text{m}}^{\circ}$ and $\Delta_{\text{cr}}^{\text{I}} H_{\text{m}}^{\circ}(T_{\text{fus}})$ as recommended by Acree and Chickos [31]. The latter sum was adjusted to the reference temperature $T = 298.15$ K with help of Equation (8) [31]:

$$\Delta_{\text{cr}}^{\text{I}} H_{\text{m}}^{\circ}(298.15 \text{ K}) / (\text{J} \cdot \text{mol}^{-1}) = \Delta_{\text{cr}}^{\text{I}} H_{\text{m}}^{\circ}(T_{\text{fus}}/\text{K}) - \left(\Delta_{\text{cr}}^{\text{g}} C_{\text{p,m}}^{\circ} - \Delta_{\text{I}}^{\text{g}} C_{\text{p,m}}^{\circ} \right) \times [(T_{\text{fus}}/\text{K}) - 298.15 \text{ K}] \quad (8)$$

where $\Delta_{\text{cr}}^{\text{g}} C_{\text{p,m}}^{\circ}$ and $\Delta_{\text{I}}^{\text{g}} C_{\text{p,m}}^{\circ}$ are given in Table S5. With this adjustment, the molar enthalpy of fusion $\Delta_{\text{cr}}^{\text{I}} H_{\text{m}}^{\circ}(298.15 \text{ K}) = 11.4 \pm 1.2$ kJ·mol^{−1} (see Table S4) of 3-methyl-indole was calculated. Uncertainty in the temperature adjustment of fusion enthalpy from T_{fus} to the reference temperature was estimated to account for 30% of the total adjustment [32]. The experimental vaporization enthalpy for 3-methyl-indole is missing in the literature. However, using the common thermochemical equation:

$$\Delta_{\text{I}}^{\text{g}} H_{\text{m}}^{\circ}(298.15 \text{ K}) = \Delta_{\text{cr}}^{\text{g}} H_{\text{m}}^{\circ}(298.15 \text{ K}) - \Delta_{\text{cr}}^{\text{I}} H_{\text{m}}^{\circ}(298.15 \text{ K}) = (81.4 - 11.4) = 70.0 \pm 1.3 \text{ kJ} \cdot \text{mol}^{-1} \quad (9)$$

it can be derived and inserted into Equations (2) and (3).

The vapor pressures of 1,2-dimethyl indole were studied for the first time. In this work, the vapor pressures of 1,2-dimethylindole were studied by the transpiration method at temperatures below and above its melting temperature. Results are given in Table 4. Values of sublimation enthalpy $\Delta_{\text{cr}}^{\text{g}} H_{\text{m}}^{\circ}(298.15 \text{ K}) = 83.2 \pm 0.7$ kJ·mol^{−1} and vaporization enthalpy $\Delta_{\text{I}}^{\text{g}} H_{\text{m}}^{\circ}(298.15 \text{ K}) = 67.6 \pm 0.7$ kJ·mol^{−1} were measured. The fusion enthalpy of 1,2-dimethylindole $\Delta_{\text{cr}}^{\text{I}} H_{\text{m}}^{\circ}(298.15 \text{ K}) = 13.3 \pm 1.1$ kJ·mol^{−1} is derived in Table S4. The difference between the sublimation and fusion enthalpies, $\Delta_{\text{I}}^{\text{g}} H_{\text{m}}^{\circ}(298.15 \text{ K}) = 69.9 \pm 1.3$ kJ·mol^{−1}, agrees with the transpiration enthalpy, $\Delta_{\text{I}}^{\text{g}} H_{\text{m}}^{\circ}(298.15 \text{ K}) = 67.6 \pm 0.7$ kJ·mol^{−1}, which proves the consistency of the data measured in this work for 1,2-dimethylindole in the solid–gas, liquid–gas and solid–liquid phase transitions.

3.3. Step III: Determination of the Missing Vaporization Enthalpies

3.3.1. Determination from Boiling Temperatures Available in the Literature at Different Pressures

Systematic vapor pressure measurements for dimethylindole derivatives are generally not found in the literature. In order to determine at least the general trends for these compounds, the experimental boiling temperatures available in the literature at different pressures [33] were collected in this work and approximated using Equation (5). The origin of these boiling points comes from the distillation of reaction mixtures after synthesis and not in special physico-chemical investigations. Usually, temperatures are given in the range of a few degrees, and pressures are measured with uncalibrated manometers. In our earlier work on methyl- and dimethyl-indoles, however, we have shown that reasonable trends can generally be derived even from such raw data [3]. The vaporization enthalpies, $\Delta_{\text{I}}^{\text{g}} H_{\text{m}}^{\circ}(298.15 \text{ K})$, obtained in this way are referred to as boiling points (BPs) and are given in Table 5 for comparison with the results determined by other methods.

3.3.2. Determination by Correlation with Retention Indices

It is well known that the $\Delta_{\text{I}}^{\text{g}} H_{\text{m}}^{\circ}(298.15 \text{ K})$ -values correlate linearly with the gas-chromatographic retention indices in a series of structurally similar compounds. We have derived a reliable linear correlation between the enthalpies of vaporization,

$\Delta_1^{\text{g}}H_{\text{m}}^{\text{o}}$ (298.15 K)-values, of compounds with reliable experimental data and the Kovats indices, J_x , available for these compounds in the literature [34] (see Table 6):

$$\Delta_1^{\text{g}}H_{\text{m}}^{\text{o}}(298.15 \text{ K}) / (\text{kJ}\cdot\text{mol}^{-1}) = 1.8 + 0.0462 \times J_x \quad \text{with } (R^2 = 0.997) \quad (10)$$

Table 6. Correlation of the vaporization enthalpies, $\Delta_1^{\text{g}}H_{\text{m}}^{\text{o}}$ (298.15 K), of cyclic aliphatic and aromatic hydrocarbons with their Kovats indices (J_x).

Compound	J_x ^a	$\Delta_1^{\text{g}}H_{\text{m}}^{\text{o}}$ (298 K) _{exp}	$\Delta_1^{\text{g}}H_{\text{m}}^{\text{o}}$ (298 K) _{calc} ^b	Δ ^c
		kJ·mol ⁻¹	kJ·mol ⁻¹	kJ·mol ⁻¹
1-methyl-pyrrolidine	697	34.2 ± 0.2 [35]	34.0	0.2
toluene	780	38.1 ± 0.2 [35]	37.8	0.3
1,4-dimethylbenzene	876	42.4 ± 0.2 [35]	42.3	0.1
indene	1059	50.6 ± 1.5 [36]	50.7	−0.1
indane	1033	49.2 ± 1.0 [36]	49.5	−0.3
tetraline	1164	55.2 ± 1.0 [35]	55.6	−0.4
quinoline	1231	59.3 ± 0.4 [4]	58.7	0.6
1-methyl-indole	1285	61.9 ± 0.3 [37]	61.2	0.7
H8-indole	1140	53.5 ± 0.7 [3]	54.5	−1.0
3-methyl-indoline	1330		63.2 ± 1.0	
3-methyl-(H8)-indole	1217		58.0 ± 1.0	

^a Kovats indices at 443 K, J_x , on the standard non-polar column SE-30. ^b Calculated using Equation (10) with the assessed expanded uncertainty of ±1.0 kJ·mol⁻¹ (0.95 level of confidence, $k = 2$). ^c Difference between columns 3 and 4 in this table.

The enthalpies of vaporization of cyclic aliphatic and aromatic hydrocarbons derived from this correlation (see Table 6, column 4) agree well with those taken from the literature for the correlation. Table 6 shows that the differences between the experimental enthalpies of vaporization and the “empirical” values calculated according to Equation (10) are mostly less than 0.5 kJ·mol⁻¹. Therefore, the uncertainties of the enthalpies of vaporization of 3-methyl-indoline and 3-methyl-(H8)-indole, estimated from the correlation of $\Delta_1^{\text{g}}H_{\text{m}}^{\text{o}}$ (298.15 K) with Kovats indices, are evaluated with an uncertainty of ±1.0 kJ·mol⁻¹.

Furthermore, reliable linear correlation between vaporization enthalpies $\Delta_1^{\text{g}}H_{\text{m}}^{\text{o}}$ (298.15 K) and the gas-chromatographic Lee indices [38], J_{Lee} , of methyl-indoles, methyl-quinolines and parent compounds (see Table S7) have been derived.

$$\Delta_1^{\text{g}}H_{\text{m}}^{\text{o}}(298.15 \text{ K}) / (\text{kJ}\cdot\text{mol}^{-1}) = 1.3 + 0.2712 \times J_{Lee} \quad \text{with } (R^2 = 0.999) \quad (11)$$

The vaporization enthalpy of 1,2-dimethyl-indole, $\Delta_1^{\text{g}}H_{\text{m}}^{\text{o}}$ (298.15 K) = 67.6 ± 1.0 kJ·mol⁻¹, derived from this correlation agrees perfectly with the value $\Delta_1^{\text{g}}H_{\text{m}}^{\text{o}}$ (298.15 K) = 67.6 ± 0.7 kJ·mol⁻¹ measured in this work. This good agreement can be seen as an additional validation of the experimental data measured in this work with the transpiration method (see Table 4).

3.3.3. Determination by Correlation with Normal Boiling Temperatures T_b

Another way to determine the missing enthalpies of vaporization is to correlate the enthalpies of vaporization, $\Delta_1^{\text{g}}H_{\text{m}}^{\text{o}}$ (298.15 K), with the normal boiling temperatures [4]. The data available in the literature on the normal boiling temperatures, T_b , of methyl-substituted indoles were correlated with the reliable $\Delta_1^{\text{g}}H_{\text{m}}^{\text{o}}$ (298.15 K)-values available from the literature. For the set of indoles compiled in Table 7, the following linear correlation between the $\Delta_1^{\text{g}}H_{\text{m}}^{\text{o}}$ (298.15 K)-values and their T_b was obtained:

$$\Delta_1^{\text{g}}H_{\text{m}}^{\text{o}}(298.15 \text{ K}) / (\text{kJ}\cdot\text{mol}^{-1}) = -91.7 + 0.2991 \times T_b \quad \text{with } (R^2 = 0.988) \quad (12)$$

Table 7. Correlation of the vaporization enthalpies $\Delta_1^{\text{g}}H_m^{\text{o}}$ (298.15 K) of indole derivatives and their T_b normal boiling temperatures.

Compound	T_b ^a K	$\Delta_1^{\text{g}}H_m^{\text{o}}$ (298.15 K) _{exp} kJ·mol ⁻¹	$\Delta_1^{\text{g}}H_m^{\text{o}}$ (298.15 K) _{calc} ^b kJ·mol ⁻¹	Δ ^c kJ·mol ⁻¹
indole	527.0	65.6 ± 0.4 [4]	65.9	−0.3
1-methyl-indole	512.6	61.9 ± 0.3 [37]	61.6	0.3
2-methyl-indole	545.2	71.7 ± 0.4 [3]	71.4	0.3
3-methyl-indole	538.7	70.1 ± 0.5 [Table 5]	69.4	0.7
5-methyl-indole	540.2	70.4 ± 0.7 [4]	69.9	0.5
7-methyl-indole	539.2	68.8 ± 0.8 [4]	69.6	−0.8
1,2-dimethyl-indole	533.5	67.6 ± 0.7 [Table 4]	67.9	−0.3
2,3-dimethyl-indole	558.2	75.2 ± 1.0 [Table 5]	75.3	−0.1
1,3-dimethyl-indole	531.7		67.3 ± 1.0	

^a Normal boiling temperatures are from [33]. ^b Calculated using Equation (12). ^c Difference between columns 3 and 4.

Table 7 shows that the differences between the experimental enthalpies of vaporization and the “empirical” values calculated according to Equation (12) are mostly less than 0.5 kJ·mol⁻¹. Therefore, the uncertainty of the enthalpy of vaporization of 1,3-dimethylindole derived from this correlation was evaluated as ±1.0 kJ·mol⁻¹.

3.3.4. Assessment of the Missing Vaporization Enthalpies by the “Centerpiece” Approach

No data on the enthalpies of vaporization of 1,2-dimethyl-(H8)-indole and 1,3-dimethyl-(H8)-indole were found in the existing literature. The enthalpies of vaporization of 3-methyl-indoline, 2,3-dimethyl-indoline, 1,2-dimethyl-indoline and 1,3-dimethyl-indoline, which were determined from the boiling temperatures at different pressures (see Section 3.3.3), also require additional validation, as they were derived from data of uncertain quality. For these estimations, the “centerpiece” approach recently developed in our work was applied.

This approach is based on the well-established principles of group additivity (GA), which are basically used for the estimation of thermodynamic properties [39]. In the conventional way, the reliable experimental vaporization enthalpies for the widest possible range of molecules are divided into relatively small groups, like “LEGO bricks”. Using a matrix calculation, a precisely defined numerical contribution is attributed to each group. The prediction of the enthalpy of vaporization is then a simple construction of the desired molecule from the “bricks”, where the energetics of a molecule is assembled from the appropriate number and type of bricks. The GA method is simple and straightforward, but it is impractical for large molecules due to there being too many “building bricks”. To overcome this drawback, a general approach was developed to assess the vaporization enthalpies based on a so-called “centerpiece” molecule.

The idea behind the “centerpiece” approach is to start the prediction with a potentially large “core” molecule with a reliable $\Delta_1^{\text{g}}H_m^{\text{o}}$ (298.15 K)-value that can generally mimic the structure of the molecule of interest. A visualization of the “centerpiece” approach to estimating $\Delta_1^{\text{g}}H_m^{\text{o}}$ (298.15 K) of 3-methyl indoline from the reliable enthalpy of vaporization of indoline is shown in Figure 3.

The CH₃-contribution estimated from reliable vaporization enthalpies of methylcyclopentane [40] and cyclopentane [40] can be considered universal in the context of this work and can be used for further estimates of the $\Delta_1^{\text{g}}H_m^{\text{o}}$ (298.15 K)-values for 2,3-dimethyl-indoline, 1,3-dimethyl-indoline, 1,2-dimethyl-(H8)-indole and 1,3-dimethyl-(H8)-indole, as shown in Figure 4.

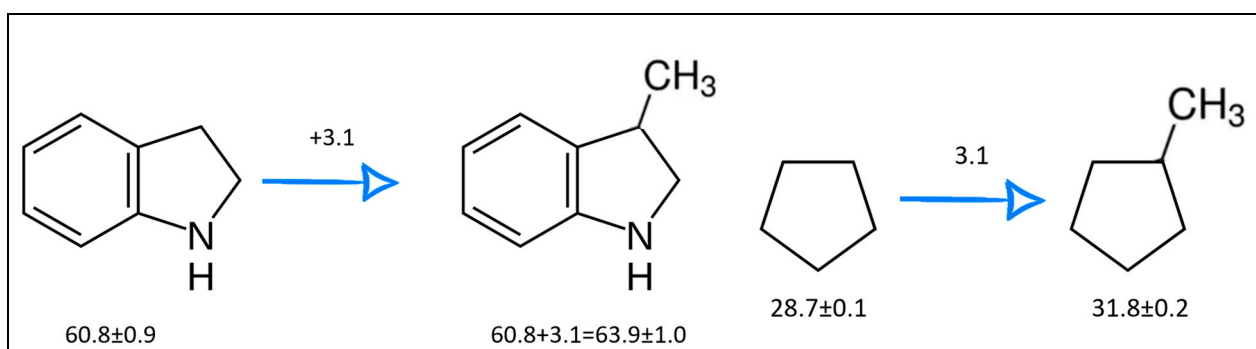


Figure 3. Left: application of the “centerpiece” approach to estimate the vaporization enthalpy of 3-methyl-indoline from the reliable enthalpy of vaporization of indoline [3]. Right: estimation of the CH₃-contribution from vaporization enthalpies of methyl-cyclopentane [40] and cyclopentane [40]. Numerical values are given in kJ·mol⁻¹ at $T = 298.15$ K.

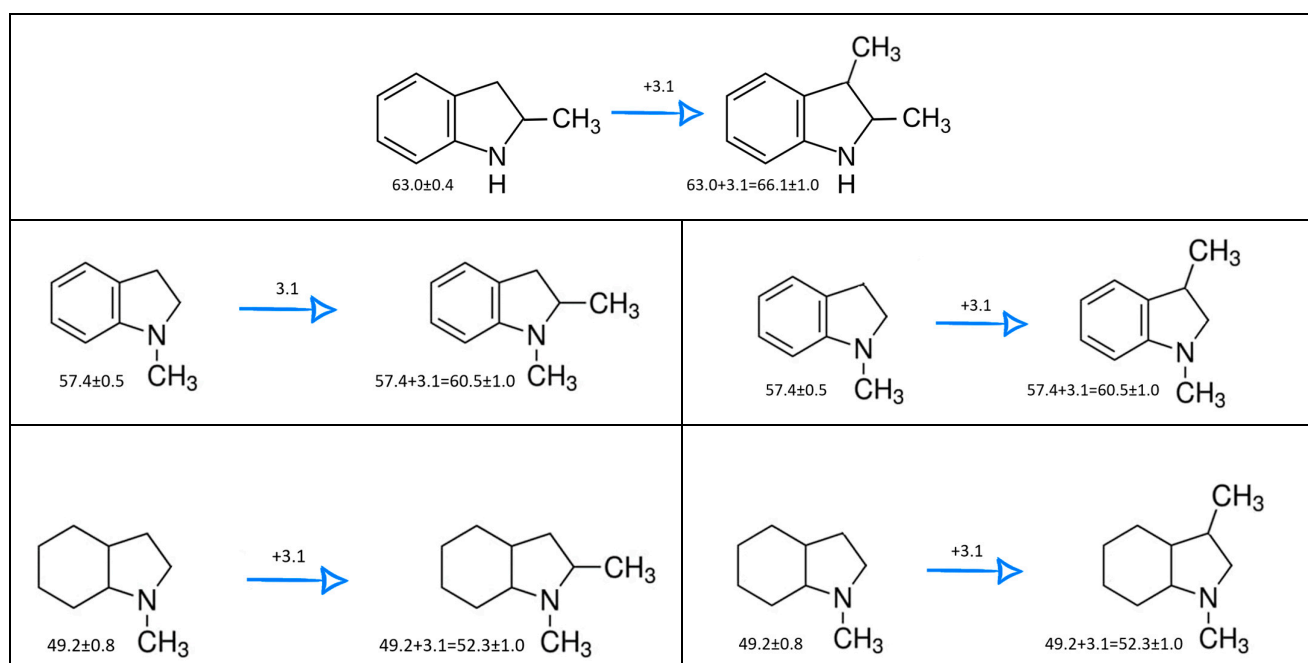


Figure 4. Application of the “centerpiece” approach to estimate the vaporization enthalpies, $\Delta_1^{\text{S}}H_m^{\text{O}}$ (298.15 K), of 2,3-dimethyl-indoline, 1,2-dimethyl-indoline, 1,3-dimethyl-indoline, 1,2-dimethyl-(H8)-indole and 1,3-dimethyl-(H8)-indole. Numerical values are given in kJ·mol⁻¹ at $T = 298.15$ K.

The “empirical” $\Delta_1^{\text{S}}H_m^{\text{O}}$ (298.15 K)-values derived in Sections 3.3.1–3.3.4 are compiled in Table 5 for comparison. It is obvious that they agree within their uncertainties for each compound. To gain more confidence in these results, the weighted average enthalpies for each indole derivative were estimated, and these values were recommended for thermochemical calculations according to Equation (2) to derive the liquid-phase enthalpies of formation for the LOHC systems based on methyl-indole derivatives.

3.4. Step IV: Liquid-Phase Standard Molar Enthalpies of Formation of HL and HR Materials

In this final step, the *gas-phase* enthalpies of formation, $\Delta_f H_m^{\text{O}}$ (g, 298.15 K), of indole derivatives derived in step I (see Table 3) were used together with the vaporization enthalpies, $\Delta_1^{\text{S}}H_m^{\text{O}}$ (298.15 K), evaluated in steps II and III, and these results were applied according to Equation (2) to obtain the *liquid-phase* $\Delta_f H_m^{\text{O}}$ (liq, 298.15 K), given in Table 8.

Table 8. Calculation of the *liquid-phase* enthalpies of formation, $\Delta_f H_m^0(\text{liq})$, of the indole derivatives, at $T = 298.15 \text{ K}$ ($p^\circ = 0.1 \text{ MPa}$, in $\text{kJ}\cdot\text{mol}^{-1}$).

Compound	$\Delta_f H_m^0(\text{Gas})^a$	$\Delta_f^g H_m^0^b$	$\Delta_f H_m^0(\text{liq})^c$
indole [3]	160.4	65.7 ± 0.6	94.7
indoline [3]	117.6	60.8 ± 0.9	56.8
H8-indole [3]	−63.5	53.5 ± 0.7	−117.0
2-methyl-indole [3]	120.2	71.7 ± 0.4	48.5
2-methyl-indoline [3]	79.4	63.0 ± 0.4	16.4
<i>trans</i> -2-methyl-(H8)-indole [3]	−100.4	57.8 ± 0.8	−158.2
3-methyl-indole	126.0	70.1 ± 0.5	55.9
3-methyl-indoline	85.8	63.8 ± 0.6	22.0
<i>trans</i> -3-methyl-(H8)-indole	−93.8	58.0 ± 0.7	−151.8
2,3-dimethylindole	86.6	75.2 ± 1.0	11.4
2,3-dimethyl-indoline	47.0	66.2 ± 1.0	−19.2
2,3-dimethyl-(H8)-indole	−120.9	61.2 ± 1.0	−182.1
1,2-dimethylindole	111.4	67.6 ± 0.5	43.8
1,2-dimethyl-indoline	72.8	60.5 ± 0.9	12.3
<i>trans</i> -1,2-dimethyl-(H8)-indole	−113.0	52.3 ± 1.0	−165.3
1,3-dimethylindole	116.3	67.5 ± 0.8	48.8
1,3-dimethyl-indoline	74.6	60.4 ± 0.9	14.2
1,3-dimethyl-(H8)-indole	−102.4	52.3 ± 1.0	−154.7

^a The G4 calculated values from Table 3. ^b Evaluated values from Table 5. ^c Calculated according to Equation (2).

With these $\Delta_f H_m^0(\text{liq}, 298.15 \text{ K})$ -values for the HL and HR materials, the energetics of the hydrogenation/dehydrogenation reactions can now be calculated according to Equation (1). For a complete overview, our recent data on unsubstituted indole derivatives and 2-methyl indole derivatives [3] are also compiled in Table 8 and discussed.

4. Discussion

4.1. Thermodynamic Analysis of LOHC Systems (Combination of Experimental and Theoretical Methods)

4.1.1. Energetics of Hydrogen Uptake and Release in the Liquid Phase

From a theoretical point of view, it is interesting to analyze the energetics of the stepwise indole hydrogenation as shown in Figure 5.

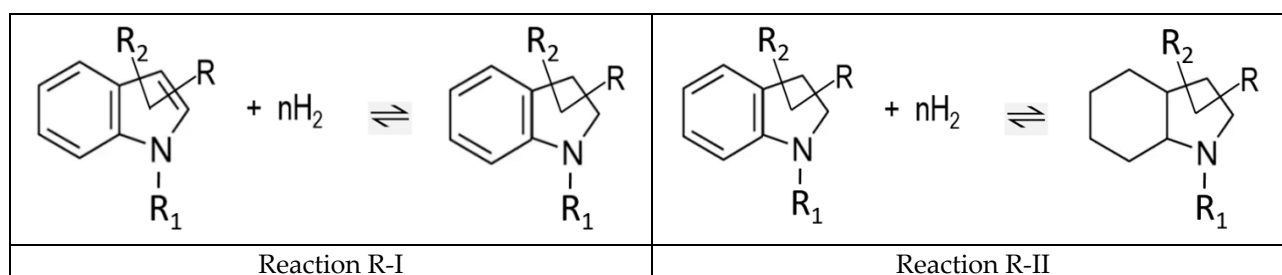


Figure 5. Reversible reactions of the partial hydrogenation (reaction R-I) and the consequent full hydrogenation of the indole derivatives (reaction R-II).

The partial hydrogenation of the double bond involved in the five-membered ring is represented by reaction R-I, and the consequent hydrogenation of all three double bonds in the six-membered ring is represented by reaction R-II.

From a practical point of view, the energetics of the complete hydrogenation of the aromatic system, represented by reaction R-III (see Figure 6), is crucial for optimizing the temperature management of a chemical reactor.

It should be noted that the reactions shown in Figures 5 and 6 represent the generalization of the individual reactions of reversible hydrogenation/dehydrogenation in the methyl-indole-based LOHC systems shown in Figure 1.

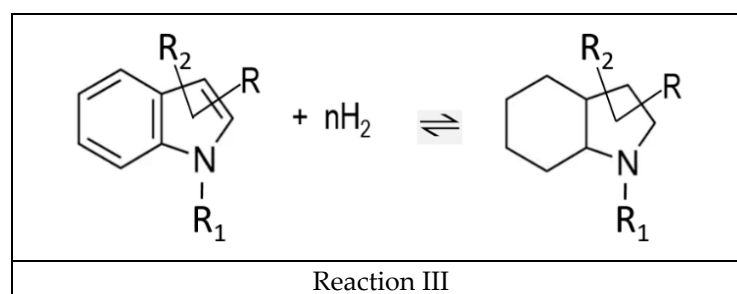


Figure 6. Reversible reactions of the full hydrogenation of the indole derivatives.

The enthalpies of the hydrogenation/dehydrogenation reactions R-I, R-II and R-III were derived according to Hess's law (see Equation (1)), using the *liquid-phase* standard molar enthalpies of formation of the reaction participants evaluated in Table 8. The *liquid-phase* enthalpies of the reversible dehydrogenation/hydrogenation reactions, $\Delta_r H_m^o(\text{liq})$, estimated according to Equation (1), are given in Table 9.

Table 9. Calculation of the *liquid-phase* reaction enthalpies, $\Delta_r H_m^o(\text{liq})$, of the hydrogenation of indole derivatives, at $T = 298.15 \text{ K}$ ($p^\circ = 0.1 \text{ MPa}$, in $\text{kJ}\cdot\text{mol}^{-1}$).

Substituents	R-I	R-II	R-III	$\Delta_r H_m^o(\text{g})/\text{H}_2$ ^e	Δ ^f
	$\Delta_r H_m^o(\text{liq})$ ^a	$\Delta_r H_m^o(\text{liq})$ ^b	$\Delta_r H_m^o(\text{liq})$ ^c		
R = R ₁ = R ₂ = H	−37.9	−173.8	−211.7	−52.9	3.1
R = 2-CH ₃ ; R ₁ = R ₂ = H	−32.1	−174.6	−206.7	−51.7	3.5
R = 3-CH ₃ ; R ₁ = R ₂ = H	−33.9	−173.8	−207.7	−51.9	3.1
R = 2-CH ₃ ; R ₁ = H; R ₂ = 3-CH ₃	−30.6	−162.9	−193.5	−48.4	3.5
R = 2-CH ₃ ; R ₁ = CH ₃ ; R ₂ = H	−31.7	−177.4	−209.1	−52.3	3.8
R = H; R ₁ = CH ₃ ; R ₂ = CH ₃	−34.8	−168.7	−203.5	−50.8	3.9

^a Calculated according to Hess's law applied to R-I using the enthalpies of formation of the reactants from Table 8.

^b Calculated according to Hess's law applied to R-II using the enthalpies of formation of the reactants from Table 8. ^c Calculated according to Hess's law applied to R-III using the enthalpies of formation of the reactants from Table 8. ^d Liquid-phase reaction enthalpy per mole H₂ calculated from data for reaction R-III in this table.

^e Gas-phase reaction enthalpy per mole H₂ calculated from data for reaction R-III in Table 10. ^f Difference between columns 5 and 6 in this table.

Table 10. Calculation of the *gas-phase* reaction enthalpies, $\Delta_r H_m^o(\text{g})$, of the hydrogenation of indole derivatives, at $T = 298.15 \text{ K}$ ($p^\circ = 0.1 \text{ MPa}$, in $\text{kJ}\cdot\text{mol}^{-1}$).

Substituents	R-I	R-II	R-III	$\Delta_r H_m^o(\text{g})/\text{H}_2$ ^d
	$\Delta_r H_m^o(\text{g})$ ^a	$\Delta_r H_m^o(\text{g})$ ^b	$\Delta_r H_m^o(\text{g})$ ^c	
R = R ₁ = R ₂ = H	−42.8	−181.1	−223.9	−56.0
R = 2-CH ₃ ; R ₁ = R ₂ = H	−40.8	−179.8	−220.6	−55.2
R = 3-CH ₃ ; R ₁ = R ₂ = H	−40.2	−179.6	−219.8	−55.0
R = 2-CH ₃ ; R ₁ = H; R ₂ = 3-CH ₃	−39.6	−167.9	−207.5	−51.9
R = 2-CH ₃ ; R ₁ = CH ₃ ; R ₂ = H	−38.6	−185.8	−224.4	−56.1
R = H; R ₁ = CH ₃ ; R ₂ = CH ₃	−41.7	−177.0	−218.7	−54.7

^a Calculated according to Hess's law applied to R-I using the enthalpies of formation of the reactants from Table 8.

^b Calculated according to Hess's law applied to R-II using the enthalpies of formation of the reactants from Table 8.

^c Calculated according to Hess's law applied to R-III using the enthalpies of formation of the reactants from Table 8. ^d Reaction enthalpy per mole H₂ calculated from data for reaction R-III.

As can be seen from this table, the hydrogenation of the double bond in the five-membered ring (reaction R-I) has an enthalpy of reaction of about $-33 \text{ kJ}\cdot\text{mol}^{-1}$ and does not differ significantly for all the structures considered in Table 9. The hydrogenation of three double bonds in the six-membered ring (reaction R-II) is more exothermic, with an enthalpy of reaction of about $-173 \text{ kJ}\cdot\text{mol}^{-1}$ or relative to the hydrogen molecules $-173/3 = -58 \text{ kJ}\cdot\text{mol}(\text{H}_2)^{-1}$. On the other hand, this means that the dehydrogenation of the six-membered ring is more energetically demanding than the dehydrogenation of the five-membered ring.

It is interesting to compare the energetics of hydrogenation of double bonds in nitrogen-containing five-membered rings and in the corresponding carbocyclic aromatic compounds (see Figure 7).

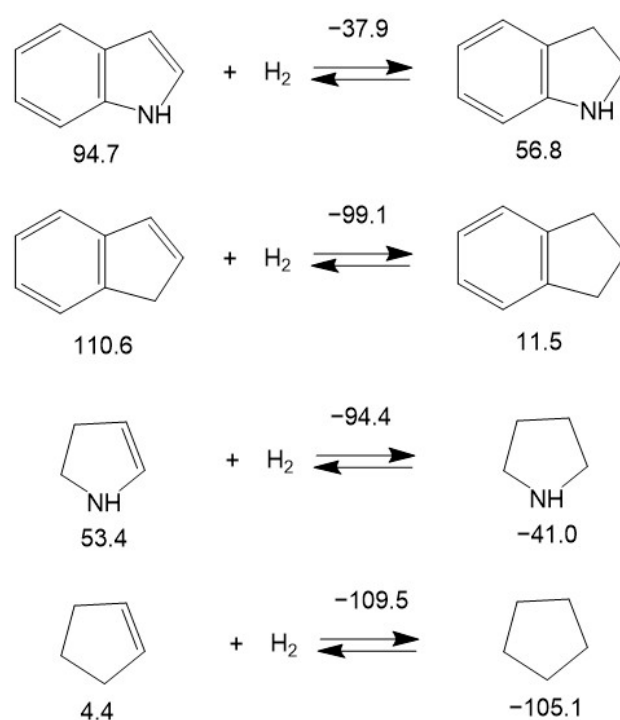


Figure 7. Comparison of the energetics of hydrogenation of double bonds in nitrogen-containing five-membered rings (indole and 2-pyrroline) and in the corresponding carbocyclic aromatic compounds (indene and cyclopentene). Figures below molecules are $\Delta_f H_m^{\circ}(\text{liq})$ taken from Table S2. Figures above the arrows are $\Delta_r H_m^{\circ}(\text{liq})$ calculated according to Equation (1). All values are in $\text{kJ}\cdot\text{mol}^{-1}$.

Hydrogenation of the double bond in the nitrogen-containing five-membered ring of indole ($-37.9 \text{ kJ}\cdot\text{mol}^{-1}$) has been found to be less than twice as exothermic than the corresponding bond in indene ($-99.1 \text{ kJ}\cdot\text{mol}^{-1}$). Surprisingly, this ratio is significantly lower in the non-aromatic counterparts: the nitrogen-containing five-membered ring of 2-pyrroline ($-94.4 \text{ kJ}\cdot\text{mol}^{-1}$) and the corresponding carbocyclic five-membered ring of cyclopentene ($-109.5 \text{ kJ}\cdot\text{mol}^{-1}$). The reason for this observation is most likely the conjugation of the π -electrons of benzene with the electronic orbitals of nitrogen. The significantly lower decrease in hydrogenation enthalpy was observed when all three double bonds in the six-membered ring of indole ($-57.9 \text{ kJ}\cdot\text{mol}^{-1}$) were consistently hydrogenated compared to indane ($-62.6 \text{ kJ}\cdot\text{mol}^{-1}$) or benzene ($-68.5 \text{ kJ}\cdot\text{mol}^{-1}$) as shown in Figure 8.

Relating the reaction enthalpy to the amount of hydrogen captured or released ($\text{kJ}\cdot\text{mol}^{-1}/\text{H}_2$) enables a comparison of the enthalpy values of LOHC systems with different stoichiometries and is therefore important from a practical point of view. These $\Delta_r H_m^{\circ}(\text{liq})\text{H}_2$ -values are given in Table 9, column 5. In these units, the hydrogenation enthalpies of mono-methylated and di-methylated indoles range between -48.4 and $-52.3 \text{ kJ}\cdot\text{mol}^{-1}/\text{H}_2$. The lowest value was found for 2,3-dimethyl-indole (see Table 9, column 5).

All other values do not differ significantly from those for unsubstituted indole, and no clear trend can be seen with regard to the position of methylation. Therefore, we can conclude that in terms of $\Delta_r H_m^{\circ}(\text{liq})\text{H}_2$ -values, all methylated and di-methylated indoles studied in this work can be considered as suitable candidates for LOHC systems.

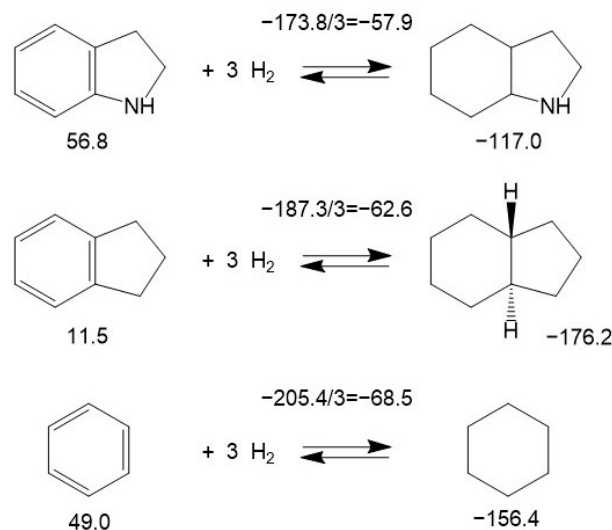


Figure 8. Comparison of the energetics of hydrogenation of three double bonds in the benzene ring of indole, in indane and in benzene. Figures below molecules are $\Delta_f H_m^{\circ}(\text{liq})$ taken from Table S2. Figures above the arrows are $\Delta_r H_m^{\circ}(\text{liq})\text{H}_2$ calculated according to Equation (1) and divided by the number of double bonds. All values are in kJ·mol⁻¹.

4.1.2. Energetics of Hydrogen Uptake and Release in an LOHC System Reacting in the Gas Phase from Pure Quantum Chemical Calculations

As a matter of fact, in order to compare the hydrogenation enthalpies, $\Delta_r H_m^{\circ}(\text{liq})\text{H}_2$, of methyl- and dimethyl-indoles in the liquid phase, four steps were taken towards these values, as mentioned in the introduction. The time-consuming work was performed to obtain and evaluate reliable enthalpies of vaporization, which combine the *gas-phase* enthalpies of formation, $\Delta_f H_m^{\circ}(\text{gas})$, and the *liquid-phase* enthalpies of formation, $\Delta_f H_m^{\circ}(\text{liq})$, of the participants in the hydrogenation reaction. How can the effort for experiments and correlations be reduced? Can some reasonable conclusions about the energetics of hydrogenation/dehydrogenation reactions perhaps already be drawn from the gas-phase enthalpies of formation, $\Delta_f H_m^{\circ}(\text{gas})$, of the reactants calculated by quantum chemical methods? In other words: how big is the difference between the $\Delta_r H_m^{\circ}(\text{liq})\text{H}_2$ -values in the *liquid phase* and the $\Delta_r H_m^{\circ}(\text{g})\text{H}_2$ -values in the *gas phase*? To answer this question, the $\Delta_r H_m^{\circ}(\text{g})\text{H}_2$ -values for reactions R-I, R-II, and R-III were calculated directly from the data given in Table 3 and the results are summarized in Table 10, column 5.

The $\Delta_r H_m^{\circ}(\text{g})\text{H}_2$ -values were found to be systematically more negative than the corresponding $\Delta_r H_m^{\circ}(\text{liq})\text{H}_2$ -values, but the difference of about 3 kJ·mol⁻¹ is almost constant (see Table 9, column 7), regardless of the position of the methyl substituents at the indole “centerpiece”. Furthermore, the *gas-phase* reaction enthalpies, $\Delta_r H_m^{\circ}(\text{g})$, of R-I, R-II and R-III (see Table 10) show the same trends compared to the corresponding *liquid-phase* enthalpies, $\Delta_r H_m^{\circ}(\text{liq})$, in Table 9. The differences between the *liquid-phase* and *gas-phase* enthalpies of the reactions of R-I, R-II and R-III (see Table S8) can be attributed to the differences in the vaporization enthalpies of the HL and HR counterparts of the LOHC systems. However, due to the structural similarity of the reactants on the left and right sides of the hydrogenation reactions, these differences can be roughly assessed and used as a correction to the quantum chemical results, when the energetics of stepwise hydrogenation are of interest.

However, for a general conclusion regarding the amount of hydrogen captured or released by the LOHC system in ($\text{kJ}\cdot\text{mol}^{-1}/\text{H}_2$)-units, the high-level QC methods provide a clear answer when a series of similarly shaped molecules are of interest.

4.2. Thermodynamic Analysis of LOHC Systems Based on Quantum Chemical Methods Only

Not only the energetics of the hydrogenation/dehydrogenation reactions are essential for optimizing hydrogen uptake and release. Since hydrogenation reactions are usually strongly exothermic, they are thermodynamically favorable at room temperature. Due to the exothermic nature of the reaction, the equilibrium can be shifted towards dehydrogenation by increasing the temperature. Therefore, the magnitude of the equilibrium constant can be helpful in locating the temperature range that is suitable for practical applications.

Can we apply modern quantum chemical calculations to determine the order of magnitude of the equilibrium constants at different temperatures and pressures? If so, the understanding of structure–property relationships and the screening of LOHC systems suitable for chemical hydrogen storage will be taken to a higher level. An algorithm leading to the equilibrium constants from QC calculations is presented below. As an example, consider the dehydrogenation of 2-methyl-H8-indole (HR material) to 2-methyl-indole (HL material) with the release of 4 moles of hydrogen, as shown in Figure 9.

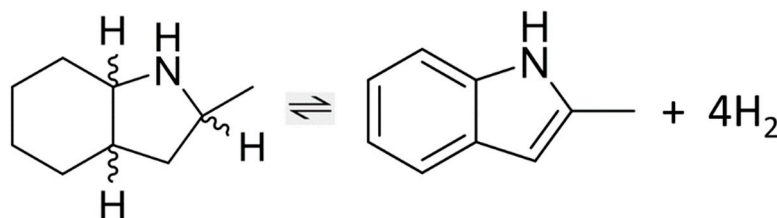


Figure 9. Dehydrogenation of 2-methyl-H8-indole to 2-methyl-indole (reaction R-IV) to release 4 moles of hydrogen.

For the general reaction “HL” + $n \times \text{H}_2 \rightarrow$ “HR”, where HL is the hydrogen-lean compound (or aromatic compound, 2-methyl-indole) and HR is the hydrogen-rich compound (fully hydrogenated aromatic compound, 2-methyl-H8-indole), the equilibrium constant K is defined as

$$K = [\text{HR}/\text{HL}] \times [P_{\text{H}_2}/p_o]^n \quad (13)$$

A pseudo-equilibrium constant, K' , is defined as

$$K' = K \times [P_{\text{H}_2}/p_o]^n \quad (14)$$

where p_o is the standard state pressure 0.1 MPa (i.e., 1 atmosphere) and K' gives the ratio of concentrations of HR to HL. The relationship between the Gibbs energy of reaction and the equilibrium constant is

$$\Delta_r G_m^\circ(T) = -RT \times \ln K \quad (15)$$

where $\ln K$ denotes the natural logarithm of K . Therefore, by rearranging Equation (15),

$$\ln K = -\Delta_r G_m^\circ(T)/RT$$

and from Equation (14),

$$\ln K' = -\Delta_r G_m^\circ(T)/RT + [n \times \ln (P_{\text{H}_2}/p_o)] \quad (16)$$

The Gibbs energy of reaction, $\Delta_r G_m^\circ$, is calculated according to Hess’s law from the Gibbs free energies of formation, $\Delta_f G_m^\circ$, of the reaction R-IV participants (2-methyl-H8-indole and 2-methyl-indole):

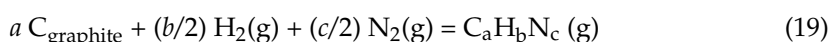
$$\Delta_r G_m^\circ = \Delta_f G_m^\circ(2\text{-methyl-indole}) + \Delta_f G_m^\circ(\text{H}_2) - \Delta_f G_m^\circ(2\text{-methyl-H8-indole}) \quad (17)$$

with $\Delta_f G_m^0(\text{H}_2) = 0 \text{ kJ}\cdot\text{mol}^{-1}$ by definition.

The basic thermodynamic equation for Gibbs energy of formation

$$\Delta_f G_m^0 = \Delta_f H_m^0 - T \times \Delta_f S_m^0 \quad (18)$$

is used to derive $\Delta_f G_m^0$ of individual compounds. The standard molar enthalpies of formation $\Delta_f H_m^0(\text{g}, 298.15 \text{ K})$ of 2-methyl-H8-indole and 2-methyl-indole can be calculated using the high-level QC method, as described in Section 3.1. The standard molar entropies, $S_m^0(\text{g}, 298.15 \text{ K})$, of 2-methyl-H8-indole and 2-methyl-indole can also be calculated using the QC method, as described in our previous work [3]. The standard molar entropies of formation, $\Delta_f S_m^0(\text{g}, 298.15 \text{ K})$, of 2-methyl-H8-indole and 2-methyl-indole were calculated based on the reaction



using the S_m^0 -values and the values of entropy of formation for elements: for $\text{C}_{\text{graphite}}$ (5.74 ± 0.13) $\text{J}\cdot\text{K}^{-1}\cdot\text{mol}^{-1}$, for $\text{H}_2(\text{g})$ (130.52 ± 0.02) $\text{J}\cdot\text{K}^{-1}\cdot\text{mol}^{-1}$, and for $\text{N}_2(\text{g})$ (191.61 ± 0.01) $\text{J}\cdot\text{K}^{-1}\cdot\text{mol}^{-1}$ recommended by Chase [41].

Thus, the Gibbs energy of formation of 2-methyl-H8-indole and 2-methyl-indole can already be calculated at the reference temperature $T = 298.15 \text{ K}$ either from the combination of the experimental and QC results or purely from the QC calculations. However, since a sufficient degree of dehydrogenation is only achieved at higher temperatures, the thermodynamic data are required at practically relevant temperatures. The ideal gas state thermodynamic properties of 2-methyl-H8-indole and 2-methyl-indole, including the standard molar heat capacities and absolute entropies of individual compounds, were calculated in the temperature range from 300 to 600 K using B3LYP hybrid density functional theory with the cc-pvtz(D3BJ) basis set with a “rigid rotator–harmonic oscillator” approach [42,43]. The essential details of the calculation are given in ESI. Results are given in Tables 11 and 12.

Table 11. Gas-phase standard molar thermodynamic properties of 2-methyl-indole at $p = 0.1 \text{ MPa}$.

T	$C_{p,m}^0(T)$	$(H_T^0 - H_{298}^0)_c$	$(H_T^0 - H_{298}^0)_e$	$S_m^0(T)_c$	$S_m^0(T)_e$	$\Delta_f H_m^0(T)$	$\Delta_f S_m^0(T)$	$\Delta_f G_m^0(T)$
K	$\text{J}\cdot\text{K}^{-1}\cdot\text{mol}^{-1}$	$\text{kJ}\cdot\text{mol}^{-1}$	$\text{kJ}\cdot\text{mol}^{-1}$	$\text{J}\cdot\text{K}^{-1}\cdot\text{mol}^{-1}$	$\text{J}\cdot\text{K}^{-1}\cdot\text{mol}^{-1}$	$\text{kJ}\cdot\text{mol}^{-1}$	$\text{J}\cdot\text{K}^{-1}\cdot\text{mol}^{-1}$	$\text{kJ}\cdot\text{mol}^{-1}$
298.15	146.1	0.0	0.0	368.8	734.7	121.6	−365.9	230.7
300	147.0	0.3	0.4	369.8	736.0	121.2	−366.2	231.0
320	156.5	3.2	5.7	379.5	751.7	115.9	−372.2	235.1
340	165.9	6.3	10.0	389.3	765.7	111.7	−376.4	239.6
360	175.1	9.7	14.4	399.1	779.4	107.2	−380.3	244.1
380	184.1	13.2	19.0	408.8	792.8	102.7	−384.0	248.6
400	192.8	16.9	24.2	418.4	804.5	97.4	−386.1	251.8
420	201.3	20.7	28.6	428.1	818.8	93.1	−390.7	257.1
440	209.4	24.7	33.6	437.6	831.4	88.0	−393.8	261.3
460	217.2	28.9	38.7	447.1	843.7	82.9	−396.6	265.3
480	224.7	33.3	44.1	456.5	855.8	77.6	−399.3	269.2
500	231.9	37.8	50.8	465.8	863.9	70.8	−398.1	269.9
520	238.8	42.4	55.1	475.0	879.1	66.5	−404.1	276.6
540	245.4	47.2	60.9	484.2	890.3	60.8	−406.1	280.1
560	251.8	52.1	66.8	493.2	901.3	54.9	−408.1	283.4
580	257.8	57.2	72.8	502.2	912.1	48.8	−409.9	286.5
600	263.7	62.4	79.8	511.0	924.0	41.9	−413.0	289.7

Table 12. Gas-phase standard molar thermodynamic properties of 2-methyl-H8-indole at $p = 0.1$ MPa.

T	$C_{p,m}^{\circ}(T)$	$(H_T^{\circ} - H_{298}^{\circ})_c$	$(H_T^{\circ} - H_{298}^{\circ})_e$	$S_m^{\circ}(T)_c$	$S_m^{\circ}(T)_e$	$\Delta_f H_m^{\circ}(T)$	$\Delta_f S_m^{\circ}(T)$	$\Delta_f G_m^{\circ}(T)$
K	J·K ⁻¹ ·mol ⁻¹	kJ·mol ⁻¹	kJ·mol ⁻¹	J·K ⁻¹ ·mol ⁻¹	J·K ⁻¹ ·mol ⁻¹	kJ·mol ⁻¹	J·K ⁻¹ ·mol ⁻¹	kJ·mol ⁻¹
298.15	178.6	0.0	0.0	368.8	1256.7	-99.3	-835.7	149.9
300	179.8	0.3	0.6	369.8	1259.0	-99.6	-836.8	151.4
320	193.0	4.1	8.1	379.5	1283.4	-103.4	-849.2	168.4
340	206.1	8.0	14.7	389.3	1304.2	-106.0	-857.9	185.7
360	219.2	12.3	21.5	399.1	1324.6	-108.5	-866.2	203.4
380	232.1	16.8	28.4	408.8	1344.5	-110.9	-873.9	221.2
400	244.8	21.6	36.1	418.4	1361.0	-113.8	-878.1	237.5
420	257.3	26.6	42.6	428.1	1382.9	-115.3	-887.8	257.5
440	269.3	31.9	50.0	437.6	1401.4	-117.4	-894.0	275.9
460	281	37.4	57.5	447.1	1419.4	-119.4	-899.8	294.5
480	292.4	43.1	65.1	456.5	1437.0	-121.3	-905.2	313.2
500	303.3	49.0	74.4	465.8	1446.5	-124.6	-902.5	326.6
520	313.9	55.2	80.9	475.0	1470.8	-125.0	-914.7	350.7
540	324.1	61.5	89.0	484.2	1487.0	-126.7	-918.9	369.5
560	333.9	68.1	97.2	493.2	1502.7	-128.4	-922.6	388.3
580	343.3	74.9	105.6	502.2	1518.0	-130.0	-926.1	407.1
600	352.4	81.8	115.1	511.0	1534.3	-132.5	-930.6	425.8

The standard molar enthalpy of formation for the compound from its elements at temperature T (taken from [44]) was calculated from Equation (20):

$$\Delta_f H_m^{\circ}(T) = \Delta_f H_m^{\circ}(298 \text{ K}) + (H_T^{\circ} - H_{298}^{\circ})_{\text{compound}} - \sum (H_T^{\circ} - H_{298}^{\circ})_{\text{elements}} \quad (20)$$

in which the summation is over the constituent elements in the compound. The standard molar entropy of formation for the compound from its elements at temperature T (taken from [44]) was calculated from Equation (21):

$$\Delta_f S_m^{\circ}(T) = S_m^{\circ}(T)_{\text{compound}} - \sum S_m^{\circ}(T)_{\text{elements}} \quad (21)$$

The standard molar Gibbs energy of formation was calculated from the following relation:

$$\Delta_f G_m^{\circ}(T) = \Delta_f H_m^{\circ}(T) - T \times \Delta_f S_m^{\circ}(T) \quad (22)$$

The temperature dependencies of the standard molar heat capacities of the gas phase calculated with the QC method were approximated by Equation (23):

$$C_{p,m}^{\circ}(T) = a + b \times T + c \times T^2 \quad (23)$$

and the approximation coefficients were used to calculate the required thermodynamic functions:

$$(H_T^{\circ} - H_{298}^{\circ}) = a \times (T - 298) + (b/2) \times (T^2 - 298^2) + (c/3) \times (T^3 - 298^3) \quad (24)$$

$$S_m^{\circ}(T) = S_m^{\circ}(298) + a \times \ln(T/298) + b \times (T - 298) + (c/2) \times (T^2 - 298^2) \quad (25)$$

The standard molar Gibbs energies of formation, $\Delta_f G_m^{\circ}(T)$, calculated according to Equation (22) for 2-methyl-H8-indole and 2-methyl-indole are given in Tables 11 and 12 (last columns). These values can now be substituted into Equation (17) to calculate the Gibbs energies of reaction, $\Delta_f G_m^{\circ}(T)$, for the reaction R-IV. The results of these calculations are summarized in Tables 13–15.

Table 13. Gas-phase standard molar Gibbs energies of 2-methyl-8H-indole and 2-methyl-indole and thermodynamic parameters of the dehydrogenation reaction R-IV at $p^\circ = 0.1$ MPa ^a.

<i>T</i>	$\Delta_f G_m^\circ(T)_{2\text{-Me-8H-Ind}}$	$\Delta_f G_m^\circ(T)_{2\text{-Me-Ind}}$	$\Delta_r G_m^\circ(T)_{\text{R-IV}}$	$\ln K'$	K'
K	$\text{kJ}\cdot\text{mol}^{-1}$	$\text{kJ}\cdot\text{mol}^{-1}$	$\text{kJ}\cdot\text{mol}^{-1}$		
298.15	149.9	230.7	80.8	−32.6	6.9×10^{-15}
300	151.4	231.3	79.9	−32.0	1.2×10^{-14}
320	168.4	238.3	69.9	−26.3	3.9×10^{-12}
340	185.7	246.0	60.2	−21.3	5.6×10^{-10}
360	203.4	253.8	50.4	−16.8	4.8×10^{-8}
380	221.2	261.7	40.5	−12.8	2.7×10^{-6}
400	237.5	268.7	31.2	−9.4	8.4×10^{-5}
420	257.5	277.8	20.3	−5.8	3.0×10^{-3}
440	275.9	286.0	10.1	−2.8	6.4×10^{-2}
460	294.5	294.2	−0.3	0.1	1.1
480	313.2	302.5	−10.7	2.7	1.5×10
500	326.6	307.6	−19.0	4.6	9.7×10
520	350.7	319.0	−31.6	7.3	1.5×10^3
540	369.5	327.2	−42.2	9.4	1.2×10^4
560	388.3	335.5	−52.8	11.3	8.4×10^4
580	407.1	343.7	−63.4	13.2	5.2×10^5
600	425.8	352.0	−73.8	14.8	2.7×10^6

^a The approximation of the $\ln K'$ -values with the linear equation $\ln K' = -28.0 \times (1000/T) + 61.1$ with $R^2 = 0.9997$.

Table 14. Gas-phase standard molar Gibbs energies of 2-methyl-8H-indole and 2-methyl-indole and thermodynamic parameters of the dehydrogenation reaction R-IV at $p^\circ = 1.0$ MPa ^a.

<i>T</i>	$\Delta_f G_m(T)_{2\text{-Me-8H-Ind}}$	$\Delta_f G_m(T)_{2\text{-Me-Ind}}$	$\Delta_r G_m(T)_{\text{R-IV}}$	$\ln K'$	K'
K	$\text{kJ}\cdot\text{mol}^{-1}$	$\text{kJ}\cdot\text{mol}^{-1}$	$\text{kJ}\cdot\text{mol}^{-1}$		
298.15	149.9	230.7	80.8	−23.4	6.9×10^{-11}
300	151.4	231.3	79.9	−22.8	1.2×10^{-10}
320	168.4	238.3	69.9	−17.1	3.9×10^{-8}
340	185.7	246.0	60.2	−12.1	5.6×10^{-6}
360	203.4	253.8	50.4	−7.6	4.8×10^{-4}
380	221.2	261.7	40.5	−3.6	2.7×10^{-2}
400	237.5	268.7	31.2	−0.2	8.4×10^{-1}
420	257.5	277.8	20.3	3.4	3.0
440	275.9	286.0	10.1	6.5	6.4×10^2
460	294.5	294.2	−0.3	9.3	1.1×10^4
480	313.2	302.5	−10.7	11.9	1.5×10^5
500	326.6	307.6	−19.0	13.8	9.7×10^5
520	350.7	319.0	−31.6	16.5	1.5×10^7
540	369.5	327.2	−42.2	18.6	1.2×10^8
560	388.3	335.5	−52.8	20.5	8.4×10^8
580	407.1	343.7	−63.4	22.4	5.2×10^9
600	425.8	352.0	−73.8	24.0	2.7×10^{10}

^a The approximation of the $\ln K'$ -values with the linear equation $\ln K' = -28.0 \times (1000/T) + 70.4$ with $R^2 = 0.9997$.

The resulting Gibbs energies of reaction; $\Delta_f G_m^\circ(T)$, at different temperatures are given in these three tables in column 4, so that the $\ln K'$ -values can now be calculated according to Equation (16). Figure 10 gives the $\ln K'$ results from Table 13 (0.1 MPa hydrogen pressure) plotted versus $1000/T$.

As shown in Figure 10, values of $\ln K'$ greater than zero (i.e., $K' > 1$) denote the thermodynamic conditions favoring 2-methyl-8H-indole formation; values less than zero (i.e., $K' < 1$) denote reaction conditions favoring 2-methyl-indole formation. An additional advantage of the thermodynamic results derived in Tables 13–15 is that they enable the assessment of the influence of pressure on the equilibrium in the LOHC system. Indeed,

according to Equation (16), the pressure increase can be screened using the $[n \times \ln(P_{\text{H}_2}/p_0)]$ -term. In Table 13, the hydrogen pressure $P_{\text{H}_2} = 0.1$ MPa was set. In Tables 14 and 15, this pressure was set to 1 MPa and 2 MPa. Analysis of the K' -results in Tables 13–15 shows that increasing the hydrogen pressure from 0.1 MPa to 2 MPa allows the dehydrogenation temperature to be reduced from 460 K to 400 K. Thus, the thermodynamic results derived in Tables 11–15 enable the optimization of the experimental conditions of hydrogenation/dehydrogenation of the LOHC systems with help of QC calculations.

Table 15. Gas-phase standard molar Gibbs energies of 2-methyl-8H-indole and 2-methyl-indole and thermodynamic parameters of the dehydrogenation reaction R-IV at $p^\circ = 2.0$ MPa ^a.

T	$\Delta_f G_m(T)_{2\text{-Me-8H-Ind}}$	$\Delta_f G_m(T)_{2\text{-Me-Ind}}$	$\Delta_r G_m(T)_{\text{R-IV}}$	$\ln K'$	K'
K	$\text{kJ}\cdot\text{mol}^{-1}$	$\text{kJ}\cdot\text{mol}^{-1}$	$\text{kJ}\cdot\text{mol}^{-1}$		
298.15	149.9	230.7	80.8	−20.62	1.1×10^{-9}
300	151.4	231.3	79.9	−20.03	2.0×10^{-9}
320	168.4	238.3	69.9	−14.28	6.3×10^{-7}
340	185.7	246.0	60.2	−9.33	8.9×10^{-5}
360	203.4	253.8	50.4	−4.86	7.7×10^{-3}
380	221.2	261.7	40.5	−0.84	4.3×10^{-1}
400	237.5	268.7	31.2	2.60	1.3
420	257.5	277.8	20.3	6.17	4.8×10^2
440	275.9	286.0	10.1	9.23	1.0×10^4
460	294.5	294.2	−0.3	12.06	1.7×10^5
480	313.2	302.5	−10.7	14.66	2.3×10^6
500	326.6	307.6	−19.0	16.56	1.6×10^7
520	350.7	319.0	−31.6	19.30	2.4×10^8
540	369.5	327.2	−42.2	21.39	2.0×10^9
560	388.3	335.5	−52.8	23.32	1.3×10^{10}
580	407.1	343.7	−63.4	25.14	8.3×10^{10}
600	425.8	352.0	−73.8	26.78	4.3×10^{11}

^a The approximation of the $\ln K'$ -values with the linear equation $\ln K' = -28.0 \times (1000/T) + 73.1$ with $R^2 = 0.9997$.

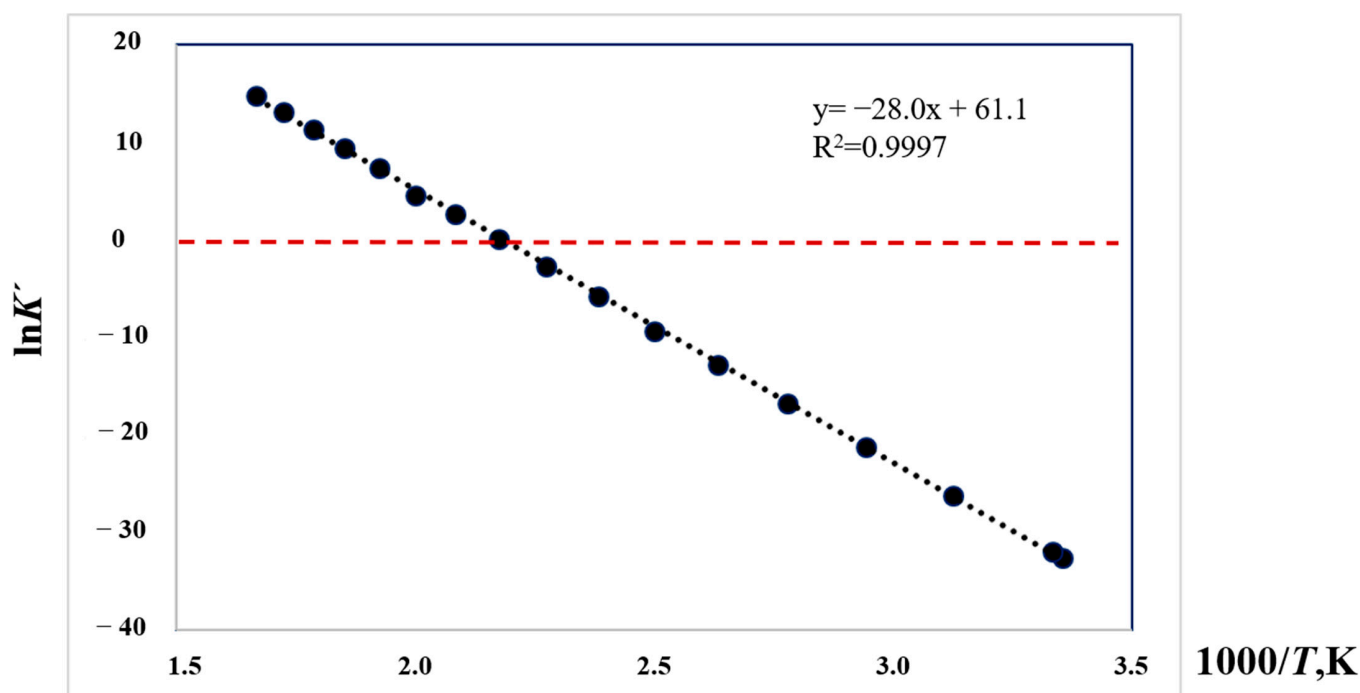


Figure 10. The $\ln K'$ values as a function of inverse temperature for the dehydrogenation of 2-methyl-8H-indole to 2-methyl-indole (calculated from the results in Table 13).

The pseudo-equilibrium constants K' calculated in Tables 13–15 can be used to assess the thermodynamic equilibrium concentrations of the hydrogen-lean and hydrogen-rich reaction products. In the ideal gas mixture of reaction participants, the partial pressure P_i of each constituent is equal to its mole fraction N_i times the total pressure P_{tot} :

$$P_i = N_i \times P_{\text{tot}} \quad (26)$$

The mole fraction is the number of moles of each constituent, n_i , divided by the total number of moles, n_{tot} , and the gas-phase constant K' can be expressed as

$$K' = K_n \left(\frac{P_{\text{tot}}}{n_{\text{tot}}} \right)^{\Delta v} \quad (27)$$

in which K_n is the equilibrium constant expressed in number of moles and Δv is the increment in number of moles of gas in the reaction; that is

$$\Delta v = \sum v_i$$

with v_i positive for products and negative for reactants. For a typical dehydrogenation of 2-methyl-H8-indole to 2-methyl-indole (reaction R-IV in Figure 9) to release 4 moles of hydrogen. the pseudo-equilibrium constant K' in the standard state is expressed as

$$K' = \frac{(n_{2\text{Me-indole}}) \cdot (n_{\text{H}_2})^4}{n_{2\text{Me-H8-indole}}} \left(\frac{1}{n_{\text{tot}}} \right)^4 \quad (28)$$

With the numerical K' values for each reaction temperature from Tables 13–15, the composition of the reaction mixture can be estimated by successive approximation.

4.3. Empirical Simplification Instead of Quantum Chemical Calculations?

The algorithm and methods for determining the thermodynamic properties of the hydrogen-poor and hydrogen-rich counterparts of the LOHC systems at the reference temperature $T = 298.15$ K are well established [45]. A reasonable combination of experimental, empirical and theoretical methods leads to reliable results for $\Delta_f H_m^\circ(298.15$ K), $\Delta_f S_m^\circ(298.15$ K), $S_m^\circ(298.15$ K) and finally for $\Delta_f G_m^\circ(298.15$ K). The determination of these thermodynamic properties at elevated temperatures is a challenging task since the calculation of the heat capacities of the ideal gases requires not only a large amount of auxiliary information, but also profound experience in such calculations. In our recent work [3], the ideal-gas heat capacities, $C_{p,m}^\circ$, of indole, indoline, H8-indole, 2-methyl-indole, 2-methyl-indoline and 2-methyl-H8-indole were calculated at different temperatures between 300 and 600 K using QC methods. It has turned out that for all these indoles the temperature dependences of the heat capacities $C_{p,m}^\circ = f(T)$ are not linear in the range 300–600 K (see Figure S2).

However, it can be noticed that the gradients for the aromatic counterparts of the LOHC systems (indole, indoline, 2-methyl-indole and 2-methyl-indoline) were not very different. The same observation was made for the aliphatic counterparts of the LOHC systems (H8-indole, 2-methyl-H8-indole); their gradients were also very similar.

It was possible to obtain the linear temperature dependencies $C_{p,m}^\circ = f(T)$ when the temperature axis was used as a logarithmic function:

$$C_{p,m}^\circ = a \cdot \ln(T) + b \quad (29)$$

where coefficients a and b are adjustable parameters. The heat capacities of the aromatic counterparts of the LOHC systems (indole, indoline, 2-methyl-indole and 2-methyl-indoline) approximated by Equation (29) are shown in Figure 11.

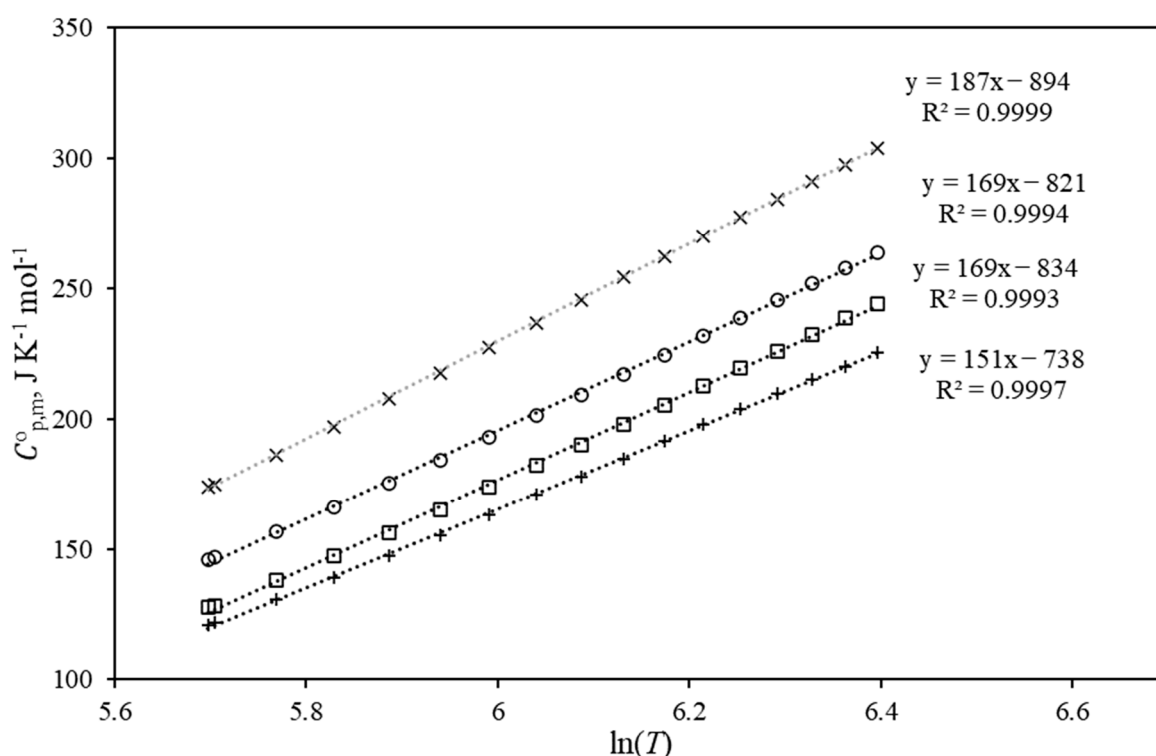


Figure 11. The gas-phase heat capacities of the aromatic counterparts of the LOHC systems approximated by Equation (29): \square —indoline, \circ —2Me-indole, \times —2-Me-indoline, $+$ —indole.

The heat capacities of the aliphatic counterparts of the LOHC systems (H8-indole, 2-methyl-H8-indole) approximated by Equation (29) are shown in Figure S2. The adjustable parameters a and b of Equation (29) and the correlation coefficient R^2 for each compound are summarized in Table 16.

Table 16. Approximation of the temperature dependence of the heat capacity of HL and HR materials by the linear equation $C_{p,m}^0 = a \cdot \ln(T) + b$.

Compound	a	b	R^2
Hydrogen-lean (HL)			
indole	151	−738	0.9997
2-Me-H-indole	169	−822	0.9994
indoline	168	−834	0.9993
2-Me-indoline	187	−894	0.9999
	169^a		
Hydrogen-rich (HR)			
H8-indole	229	−1157	0.9980
2Me-H8-indole	250	−1253	0.9982
	240^a		

^a Averaged values recommended for calculations.

As can be seen from Table 16, the coefficients representing the slopes of the temperature dependence of the heat capacity for aromatic materials are in fair agreement. The average value $a = 169$ was taken as a constant parameter for this type of material. For fully hydrogenated indoles (2Me-8H-indole and 8H-indole), the fluctuation of the a -values can also be considered acceptable, and the average value $a = 240$ was assumed as a constant parameter for fully hydrogenated indoles. To prove the validity of these assumptions, the heat capacity values for all six indoles were calculated using Equation (29) with the fixed a -parameters. These estimates agree well with the original data (see Tables S9–S14).

It can be assumed that the a -parameters are also applicable to other types of HR and HL materials (e.g., alkyl-indoles, alkyl-quinolines, alkyl-carbazoles). To apply this simplified method, only $C_{p,m}^o(298.15\text{ K})$ has to be calculated either with QC methods or with GA methods (e.g., those developed by Benson [39] or by Domalski [46]). With this numerical $C_{p,m}^o(298.15\text{ K})$ -value, the parameter b from Equation (29) is first determined at 298.15 K. Then the $C_{p,m}^o = f(T)$ -values for the range of practically relevant temperatures can be estimated. Consequently, these ideal-gas heat capacities can be used in combination with the thermodynamic data at the reference temperature to calculate the K' -values, as shown in Section 4.2, which help to optimize the hydrogenation/dehydrogenation reaction conditions.

5. Conclusions

A consistent dataset for the thermochemical properties of methyl-substituted indoles has been determined by an approach based on different methods for mutual validation: Experimental measurements utilizing combustion calorimetry and differential scanning calorimetry have been combined with quantum chemical methods and a group-additivity approach. The results confirmed the lower enthalpy of reaction for dehydrogenation in the five-membered ring and the positive effect of lower enthalpy of reaction by the addition of the nitrogen-heteroatom compared to the corresponding homocyclic compound. However, methylation of the indole molecule also has a namable effect on the energetics of the reaction. The overall enthalpy of reaction varies within a range of $18.2\text{ kJ}\cdot\text{mol}^{-1}$ (corresponding to $4.6\text{ kJ}\cdot\text{mol}(\text{H}_2^{-1})$). The results show that both the degree of methylation and the position of the methyl groups can have a significant influence on the enthalpy of reaction. This not only influences the heat demand for hydrogen release, but also influences the reaction conditions as it influences the equilibrium constant.

Supplementary Materials: The following supporting information can be downloaded at: <https://www.mdpi.com/article/10.3390/ma16072924/s1>, Figure S1: Calculation of vaporisation enthalpy of 2-pyrroline; Figure S2: Temperature dependence of the gas-phase standard molar heat capacities; Figure S3: Dependence of the gas-phase standard molar heat capacity on $\ln(T)$; Table S1: Provenance, purity, and methods of purification of samples used in this work; Table S2: Reference values for $\Delta_f H_m^o(298.15\text{ K})$ used for thermochemical calculations at $T = 298.15\text{ K}$ ($p^\circ = 0.1\text{ MPa}$, in $\text{kJ}\cdot\text{mol}^{-1}$); Table S3: The enthalpies of homodesmotic reactions (see Figure 5) involving 3-methyl-indole $\Delta_r H_m^o(\text{g})$ at $T = 298.15\text{ K}$ ($p^\circ = 0.1\text{ MPa}$, in $\text{kJ}\cdot\text{mol}^{-1}$); Table S4: Thermodynamics of phase transitions of indole derivatives (in $\text{kJ}\cdot\text{mol}^{-1}$); Table S5: Compilation of data on molar heat capacities $C_{p,m}^o(\text{cr or liq})$ and heat capacity differences $\Delta_{\text{cr,l}}^g C_{p,m}^o$ (in $\text{J}\cdot\text{K}^{-1}\cdot\text{mol}^{-1}$) at $T = 298.15\text{ K}$; Table S6: Vapor pressures, p_i , at different temperatures compiled from the literature, standard molar vaporisation enthalpies, $\Delta_1^g H_m^o$, and standard molar vaporisation entropies, $\Delta_1^g S_m^o$; Table S7: Correlation of vaporization enthalpies, $\Delta_1^g H_m^o(298.15\text{ K})$, of aromatic hydrocarbons with their Lee's indices (J_{Lee}); Table S8: Difference in energetics between the liquid-phase reaction enthalpies, $\Delta_r H_m^o(\text{liq})$, and the gas-phase reaction enthalpies, $\Delta_r H_m^o(\text{g})$, of the hydrogenation of indole derivatives, at $T = 298.15\text{ K}$ ($p^\circ = 0.1\text{ MPa}$, in $\text{kJ}\cdot\text{mol}^{-1}$); Table S9. Gas-phase standard molar thermodynamic properties of 2-methyl-indole and 2-methyl-H8-indole at $T = 298.15\text{ K}$; Table S10: The gas-phase standard molar heat capacity, $C_{p,m}^o$, of indole; Table S11: The gas-phase standard molar heat capacity, $C_{p,m}^o$, of indoline; Table S12: The gas-phase standard molar heat capacity, $C_{p,m}^o$, of 8H-indole; Table S13: The gas-phase standard molar heat capacity, $C_{p,m}^o$, of 2Me-indole; Table S14: The gas-phase standard molar heat capacity, $C_{p,m}^o$, of 2-Me-indoline; Table S15: The gas-phase standard molar heat capacity, $C_{p,m}^o$, of 2Me-8H-indole; Transpiration method; Thermodynamics of vaporisation/sublimation; Temperature adjustments of sublimation/vaporisation enthalpies; Computation of the thermodynamic properties for studied compounds in ideal gas state. Refs. [47–61] are mentioned in the Supplementary Materials.

Author Contributions: Conceptualization, S.P.V.; methodology, P.W. and K.M.; software, A.A.S. and V.V.T.; validation, S.V.V., V.V.T. and S.P.V.; formal analysis, P.W., K.M. and S.P.V.; investigation, S.V.V.; resources, P.W. and K.M.; data curation, P.W., K.M. and S.P.V.; writing—original draft preparation, S.P.V., P.W. and K.M.; writing—review and editing, S.P.V. and V.V.T.; visualization, S.P.V. and A.A.S.;

supervision, S.P.V.; project administration, S.P.V.; funding acquisition, S.P.V. All authors have read and agreed to the published version of the manuscript.

Funding: The work was supported by the Ministry of Science and Higher Education of the Russian Federation (theme No. AAAA-A12-1111100072-9) as part of the state task of the Samara State Technical University (creation of new youth laboratories). A.A.S. gratefully acknowledges a research scholarship from the DAAD (Deutscher Akademischer Austauschdienst). This paper has been supported by the Kazan Federal University Strategic Academic Leadership Program (“PRIORITY-2030”).

Institutional Review Board Statement: Not applicable.

Informed Consent Statement: Not applicable.

Data Availability Statement: Not applicable.

Conflicts of Interest: The authors declare no conflict of interest.

References

1. Wei, D.; Shi, X.; Qu, R.; Junge, K.; Junge, H.; Beller, M. Toward a Hydrogen Economy: Development of Heterogeneous Catalysts for Chemical Hydrogen Storage and Release Reactions. *ACS Energy Lett.* **2022**, *7*, 3734–3752. [[CrossRef](#)]
2. Allendorf, M.D.; Stavila, V.; Snider, J.L.; Witman, M.; Bowden, M.E.; Brooks, K.; Tran, B.L.; Autrey, T. Challenges to developing materials for the transport and storage of hydrogen. *Nat. Chem.* **2022**, *14*, 1214–1223. [[CrossRef](#)]
3. Konnova, M.E.; Li, S.; Bösmann, A.; Müller, K.; Wasserscheid, P.; Andreeva, I.V.; Turovtzev, V.V.; Zaitsau, D.H.; Pimerzin, A.A.; Verevkin, S.P. Thermochemical Properties and Dehydrogenation Thermodynamics of Indole Derivates. *Ind. Eng. Chem. Res.* **2020**, *59*, 20539–20550. [[CrossRef](#)]
4. Safronov, S.P.; Vostrikov, S.V.; Samarov, A.A.; Wasserscheid, P.; Müller, K.; Verevkin, S.P. Comprehensive thermodynamic study of substituted indoles/perhydro indoles as potential liquid organic hydrogen carrier system. *Fuel* **2023**, *331*, 125764. [[CrossRef](#)]
5. Bachmann, P.; Schwarz, M.; Steinhauer, J.; Späth, F.; Düll, F.; Bauer, U.; Silva, T.N.; Mohr, S.; Hohner, C.; Scheuermeyer, M.; et al. Dehydrogenation of the Liquid Organic Hydrogen Carrier System Indole/Indoline/Octahydroindole on Pt(111). *J. Phys. Chem. C* **2018**, *122*, 4470–4479. [[CrossRef](#)]
6. Inman, M.; Moody, C.J. Indole synthesis—Something old, something new. *Chem. Sci.* **2013**, *4*, 29–41. [[CrossRef](#)]
7. Gribble, G.W. Recent developments in indole ring synthesis—Methodology and applications. *J. Chem. Soc. Perkin Trans. 1* **2000**, *7*, 1045–1075. [[CrossRef](#)]
8. Cacchi, S.; Fabrizi, G. Synthesis and Functionalization of Indoles Through Palladium-catalyzed Reactions. *Chem. Rev.* **2005**, *105*, 2873–2920. [[CrossRef](#)]
9. Humphrey, G.R.; Kueth, J.T. Practical Methodologies for the Synthesis of Indoles. *Chem. Rev.* **2006**, *106*, 2875–2911. [[CrossRef](#)]
10. Nelson, D.L.; Cox, M.C. *Principles of Biochemistry*, 4th ed.; W. H. Freeman and Company: New York, NY, USA, 2005.
11. Li, L.; Yang, M.; Dong, Y.; Mei, P.; Cheng, H. Hydrogen storage and release from a new promising Liquid Organic Hydrogen Storage Carrier (LOHC): 2-methylindole. *Int. J. Hydrogen Energy* **2016**, *41*, 16129–16134. [[CrossRef](#)]
12. Yang, M.; Cheng, G.; Xie, D.; Zhu, T.; Dong, Y.; Ke, H.; Cheng, H. Study of hydrogenation and dehydrogenation of 1-methylindole for reversible onboard hydrogen storage application. *Int. J. Hydrogen Energy* **2018**, *43*, 8868–8876. [[CrossRef](#)]
13. Dong, Y.; Yang, M.; Li, L.; Zhu, T.; Chen, X.; Cheng, H. Study on reversible hydrogen uptake and release of 1,2-dimethylindole as a new liquid organic hydrogen carrier. *Int. J. Hydrogen Energy* **2019**, *44*, 4919–4929. [[CrossRef](#)]
14. Dong, Y.; Zhao, H.; Zhao, Y.; Yang, M.; Zhang, H.; Cheng, H. Study of catalytic hydrogenation and dehydrogenation of 2,3-dimethylindole for hydrogen storage application. *RSC Adv.* **2021**, *11*, 15729–15737. [[CrossRef](#)] [[PubMed](#)]
15. Vostrikov, S.V.; Konnova, M.E.; Turovtzev, V.V.; Müller, K.; Verevkin, S.P. Thermodynamics of hydrogen storage: Equilibrium study of the LOHC system indole/octahydroindole. *Fuel* **2023**, *335*, 127025. [[CrossRef](#)]
16. Verevkin, S.P.; Samarov, A.A. Thermochemistry in the twenty-first century—quo vadis? In silico assisted diagnostics of available thermochemical data. *Struct. Chem.* **2023**, *34*, 285–305. [[CrossRef](#)]
17. Curtiss, L.A.; Redfern, P.C.; Raghavachari, K.; Rassolov, V.; Pople, J.A. Gaussian-3 theory using reduced Moller-Plesset order. *J. Chem. Phys.* **1999**, *110*, 4703–4709. [[CrossRef](#)]
18. Curtiss, L.A.; Redfern, P.C.; Raghavachari, K. Gaussian-4 theory. *J. Chem. Phys.* **2007**, *126*, 084108. [[CrossRef](#)] [[PubMed](#)]
19. Ochterski, J.W.; Petersson, G.A.; Montgomery, J.A. A complete basis set model chemistry. V. Extensions to six or more heavy atoms. *J. Chem. Phys.* **1996**, *104*, 2598–2619. [[CrossRef](#)]
20. Frisch, M.J.; Trucks, G.W.; Schlegel, H.B.; Scuseria, G.E.; Robb, M.A.; Cheeseman, J.R.; Scalmani, G.; Barone, V.; Petersson, G.A.; Nakatsuji, H.; et al. *Gaussian 16, Revision C.01*; Gaussian Inc.: Wallingford, CT, USA, 2016.
21. Verevkin, S.P.; Emel’yanenko, V.N.; Notario, R.; Roux, M.V.; Chickos, J.S.; Liebman, J.F. Rediscovering the Wheel. Thermochemical Analysis of Energetics of the Aromatic Diazines. *J. Phys. Chem. Lett.* **2012**, *3*, 3454–3459. [[CrossRef](#)]
22. Verevkin, S.P.; Emel’yanenko, V.N. Transpiration method: Vapor pressures and enthalpies of vaporization of some low-boiling esters. *Fluid Phase Equilibria* **2008**, *266*, 64–75. [[CrossRef](#)]

23. Zaitseva, K.V.; Emel'yanenko, V.N.; Agapito, F.; Pimerzin, A.A.; Varfolomeev, M.A.; Verevkin, S.P. Benchmark thermochemistry of methylbenzonitriles: Experimental and theoretical study. *J. Chem. Thermodyn.* **2015**, *91*, 186–193. [CrossRef]
24. Da Silva, M.A.V.R.; Cabral, J.I.T.A.; Gomes, J.R.B. Combined experimental and computational study of the energetics of methylindoles. *J. Chem. Thermodyn.* **2009**, *41*, 1193–1198. [CrossRef]
25. Good, W.D. Enthalpies of combustion of nine organic nitrogen compounds related to petroleum. *J. Chem. Eng. Data* **1972**, *17*, 28–31. [CrossRef]
26. Pracht, P.; Bohle, F.; Grimme, S. Automated exploration of the low-energy chemical space with fast quantum chemical methods. *Phys. Chem. Chem. Phys.* **2020**, *22*, 7169–7192. [CrossRef]
27. Petersson, G.A.; Bennett, A.; Tensfeldt, T.G.; Al-Laham, M.A.; Shirley, W.A.; Mantzaris, J. A complete basis set model chemistry. I. The total energies of closed-shell atoms and hydrides of the first-row elements. *J. Chem. Phys.* **1988**, *89*, 2193–2218. [CrossRef]
28. Verevkin, S.P.; Sazonova, A.Y.; Emel'yanenko, V.N.; Zaitsau, D.H.; Varfolomeev, M.A.; Solomonov, B.N.; Zherikova, K.V. Thermochemistry of Halogen-Substituted Methylbenzenes. *J. Chem. Eng. Data* **2015**, *60*, 89–103. [CrossRef]
29. Stephenson, R.M.; Malanowski, S. *Handbook of the Thermodynamics of Organic Compounds*; Springer: Dordrecht, The Netherlands, 1987; ISBN 978-94-010-7923-5.
30. Stull, D.R. Vapor Pressure of Pure Substances. Organic and Inorganic Compounds. *Ind. Eng. Chem.* **1947**, *39*, 517–540. [CrossRef]
31. Acree, W.; Chickos, J.S. Phase Transition Enthalpy Measurements of Organic and Organometallic Compounds. Sublimation, Vaporization and Fusion Enthalpies from 1880 to 2010. *J. Phys. Chem. Ref. Data* **2010**, *39*, 043101. [CrossRef]
32. Gobble, C.; Chickos, J.; Verevkin, S.P. Vapor Pressures and Vaporization Enthalpies of a Series of Dialkyl Phthalates by Correlation Gas Chromatography. *J. Chem. Eng. Data* **2014**, *59*, 1353–1365. [CrossRef]
33. SciFinder—Chemical Abstracts Service. Available online: <http://scifinder.cas.org/> (accessed on 7 February 2023).
34. Toth, T.; Borsodi, A. Gas-chromatographic retention and chemical structure. I. Correlations between the retention indexes of five-membered cyclic compounds of different saturation, containing one nitrogen atom. *Magy. Kem. F.* **1971**, *77*, 576–587.
35. Pedley, J.B.; Naylor, R.D.; Kirby, S.P. *Thermochemical Data of Organic Compounds*; Chapman and Hall: New York, NY, USA, 1986; pp. 1–792.
36. Roux, M.V.; Temprado, M.; Chickos, J.S.; Nagano, Y. Critically evaluated thermochemical properties of polycyclic aromatic hydrocarbons. *J. Phys. Chem. Ref. Data* **2008**, *37*, 1855–1996. [CrossRef]
37. Almeida, A.R.R.P.; Monte, M.J.S. Vapour pressures of 1-methyl derivatives of benzimidazole, pyrazole and indole. The energy of the intermolecular hydrogen bond NH...N. *J. Chem. Thermodyn.* **2014**, *77*, 46–53. [CrossRef]
38. Vassilaros, D.L.; Kong, R.C.; Later, D.W.; Lee, M.L. Linear retention index system for polycyclic aromatic compounds. *J. Chromatogr. A* **1982**, *252*, 1–20. [CrossRef]
39. Benson, S.W. *Thermochemical Kinetics*, 2nd ed.; John Wiley & Sons: New York, NY, USA, 1976; pp. 1–320.
40. Majer, V.; Svoboda, V. *Enthalpies of Vaporization of Organic Compounds: A Critical Review and Data Compilation*; Blackwell Scientific Publications: Oxford, UK, 1985.
41. Chase, M.W. NIST-JANAF Thermochemical Tables. 4th Edition. *J. Phys. Chem. Ref. Data Monogr.* **1998**, *9*, 1.
42. Rappoport, D.; Furche, F. Property-optimized Gaussian basis sets for molecular response calculations. *J. Chem. Phys.* **2010**, *133*, 134105. [CrossRef] [PubMed]
43. Grimme, S.; Ehrlich, S.; Goerigk, L. Effect of the damping function in dispersion corrected density functional theory. *J. Comput. Chem.* **2011**, *32*, 1456–1465. [CrossRef] [PubMed]
44. Stull, R.D.; Westrum, E.F.; Sinke, G.C. *The Chemical Thermodynamics of Organic Compounds*; Wiley: New York, NY, USA, 1969.
45. Verevkin, S.P. *Gibbs Energy and Helmholtz Energy: Liquids, Solutions and Vapours*; Wilhelm, E., Letcher, T.M., Eds.; Royal Society of Chemistry: Cambridge, UK, 2021; ISBN 978-1-83916-201-5.
46. Domalski, E.S.; Hearing, E.D. Estimation of the Thermodynamic Properties of C-H-N-O-S-Halogen Compounds at 298.15 K. *J. Phys. Chem. Ref. Data* **1993**, *22*, 805–1159. [CrossRef]
47. Dorofeeva, O.V.; Filimonova, M.A.; Marochkin, I.I. Aliphatic Amines: A Critical Analysis of the Experimental Enthalpies of Formation by Comparison with Theoretical Calculations. *J. Chem. Eng. Data* **2019**, *64*, 5630–5647. [CrossRef]
48. Verevkin, S.P. Thermochemical Investigation on α -Methyl-Styrene and Parent Phenyl Substituted Alkenes. *Thermochim. Acta* **1999**, *326*, 17–25. [CrossRef]
49. Dean, B.D.; Truce, W.E. Oxidative Conversions of Sulfene-Cycloadducts from Azaheptafulvenes and from Tropone to 1,2-Disubstituted Indoles and 2-Aryl-Benzofurans, Respectively. *J. Org. Chem.* **1981**, *46*, 3575–3576. [CrossRef]
50. Sigma-Aldrich. Available online: <https://www.sigmaaldrich.com/> (accessed on 7 February 2023).
51. Abdelaziz, A.; Zaitsau, D.H.; Kuratieva, N.V.; Verevkin, S.P.; Schick, C. Melting of Nucleobases. Getting the Cutting Edge of “Walden’s Rule”. *Phys. Chem. Chem. Phys.* **2019**, *21*, 12787–12797. [CrossRef] [PubMed]
52. Walden, P. Über Die Schmelzwärme, Spezifische Kohäsion und Molekulargrösse Bei Der Schmelztemperatur. *Z. Elektrotechnik Elektrochem.* **1908**, *14*, 713–724. [CrossRef]
53. Nagrimanov, R.N.; Ziganshin, M.A.; Solomonov, B.N.; Verevkin, S.P. Thermochemistry of Drugs: Experimental and Theoretical Study of Analgesics. *Struct. Chem.* **2019**, *30*, 247–261. [CrossRef]
54. Verevkin, S.P.; Emel'yanenko, V.N.; Nagrimanov, R.N. Nearest-Neighbor and Non-Nearest-Neighbor Interactions between Substituents in the Benzene Ring. Experimental and Theoretical Study of Functionally Substituted Benzamides. *J. Phys. Chem. A* **2016**, *120*, 9867–9877. [CrossRef] [PubMed]

55. Chickos, J.S.; Hosseini, S.; Hesse, D.G.; Liebman, J.F. Heat Capacity Corrections to a Standard State: A Comparison of New and Some Literature Methods for Organic Liquids and Solids. *Struct. Chem.* **1993**, *4*, 271–278. [[CrossRef](#)]
56. Acree, W.; Chickos, J.S. Phase Transition Enthalpy Measurements of Organic and Organometallic Compounds and Ionic Liquids. Sublimation, Vaporization, and Fusion Enthalpies from 1880 to 2015. Part 2. C11-C192. *J. Phys. Chem. Ref. Data* **2017**, *46*, 013104. [[CrossRef](#)]
57. Kulikov, D.; Verevkin, S.P.; Heintz, A. Determination of Vapor Pressures and Vaporization Enthalpies of the Aliphatic Branched C 5 and C 6 Alcohols. *J. Chem. Eng. Data* **2001**, *46*, 1593–1600. [[CrossRef](#)]
58. Emel'yanenko, V.N.; Verevkin, S.P. Benchmark Thermodynamic Properties of 1,3-Propanediol: Comprehensive Experimental and Theoretical Study. *J. Chem. Thermodyn.* **2015**, *85*, 111–119. [[CrossRef](#)]
59. Chickos, J.S.; Acree, W.E. Enthalpies of Vaporization of Organic and Organometallic Compounds, 1880–2002. *J. Phys. Chem. Ref. Data* **2003**, *32*, 519–878. [[CrossRef](#)]
60. Grimme, S. Exploration of Chemical Compound, Conformer, and Reaction Space with Meta-Dynamics Simulations Based on Tight-Binding Quantum Chemical Calculations. *J. Chem. Theory Comput.* **2019**, *15*, 2847–2862. [[CrossRef](#)] [[PubMed](#)]
61. NIST Chemistry WebBook. Available online: <https://webbook.nist.gov/chemistry/> (accessed on 7 February 2023).

Disclaimer/Publisher's Note: The statements, opinions and data contained in all publications are solely those of the individual author(s) and contributor(s) and not of MDPI and/or the editor(s). MDPI and/or the editor(s) disclaim responsibility for any injury to people or property resulting from any ideas, methods, instructions or products referred to in the content.